



Showcasing research from Assistant Professor Asma Ghazzy's laboratory, Pharmacological and Diagnostic Research Centre, Faculty of Pharmacy, Al-Ahliyya Amman University, Amman, Jordan.

Magnetic iron oxide-based nanozymes: from synthesis to application

This comprehensive review article provides a thorough overview of Iron Oxide Nanozymes (IONzymes), magnetic nanoparticles that mimic natural enzyme activities. Spotting their remarkable stability, magnetic properties, and biocatalytic capabilities, moreover, the article demonstrates various synthesis methods, including chemical, physical, and biological processes. This review also discusses the current applications of IONzymes in biomedicine, environmental fields, and the potential promising applications.

As featured in:



See Asma Ghazzy *et al.*,  
*Nanoscale Adv.*, 2024, **6**, 1611.

Cite this: *Nanoscale Adv.*, 2024, 6, 1611

# Magnetic iron oxide-based nanozymes: from synthesis to application

Asma Ghazzy, <sup>a</sup>\* Hamdi Nsairat, <sup>a</sup> Rana Said, <sup>a</sup> Obada A. Sibai, <sup>a</sup>  
Aseel AbuRuman, <sup>a</sup> Alaa S. Shraim <sup>b</sup> and Afnan Al hunaiti <sup>c</sup>

Iron oxide nanozymes (IONzymes) are a class of magnetic nanoparticles that mimic the enzymatic activity of natural enzymes. These particles have received significant attention in recent years due to their unique properties, such as high stability, tunable magnetic responsiveness, and ability to act as biocatalysts for various chemical reactions. In this review, we aim to provide an overview of the production methods of magnetic nanozymes, including chemical, physical, and biological synthesis. The structure and design of magnetic nanozymes are also discussed in detail, as well as their applications in various fields such as biomedicine and environmental science. The results of various studies and the latest advances in the field of magnetic nanozymes are also discussed. This review provides valuable insights into the current state of magnetic nanozymes and highlights their potential for further development and application in various fields.

Received 19th October 2023  
Accepted 24th January 2024

DOI: 10.1039/d3na00903c

rsc.li/nanoscale-advances

## 1. Introduction

The advancement of nanotechnology over the past two decades has highlighted new prospects in a wide range of industries due to the extraordinary qualities and distinct structure of

nanomaterials.<sup>1,2</sup> The structure of nanomaterials is divided into three layers (surface, shell, and core) where functional groups, including metal ions, tiny compounds, surfactants, and polymers, distinguish one layer from another.<sup>3,4</sup> In general, the core is the nanoparticles (NPs), which can bond with various structures and macromolecules such as composites, metal organic frameworks (MOFs), polymers, and carbon nanotubes. This diversity enhances their unique properties in terms of size, shape, composition, and structural framework, which require optimization through synthesis procedures.<sup>5–8</sup>

Metallic nanoparticles represent a corner stone in the preparation of nanomaterials.<sup>9,10</sup> Various metal oxides such as FeO,

<sup>a</sup>Pharmacological and Diagnostic Research Center, Faculty of Pharmacy, Al-Ahliyya Amman University, Amman 19328, Jordan. E-mail: a.alghazzy@ammanu.edu.jo; Tel: +962 77 7721721

<sup>b</sup>Department of Medical Laboratory Sciences, Faculty of Allied Medical Sciences, Al-Ahliyya Amman University, Amman 19328, Jordan

<sup>c</sup>Department of Chemistry, University of Jordan, Amman 11942, Jordan



Asma Ghazzy

research focus is in the areas of photocatalysis, molecular sensors, and synthesis methodologies. Dr Ghazzy has made notable contributions, publishing her work in prestigious journals. She possesses expertise in instrumental analysis techniques and using chemical software.

Dr Asma Ghazzy, a Jordanian national, obtained her PhD in Inorganic Chemistry from the University of Jordan in 2018. She has undertaken several research visits to the Technical University of Chemnitz. Currently, she is working as an Assistant Professor in the Faculty of Pharmacy at Al-Ahliyya Amman University. Dr Ghazzy previously earned her Master's Degree in Applied Chemistry. Her primary



Hamdi Nsairat

aptamers, and targeting ligands. Hamdi has published innovative works in reputable journals and possesses excellent skills in instrumental analysis and chemical software applications.

Dr Hamdi Nsairat, a Jordanian national, earned his PhD in Biophysical and Pharmaceutical Chemistry from the University of Jordan in 2020. Currently, he is an Assistant Professor at Al Ahliyya Amman University's Faculty of Pharmacy, where he has over ten years of teaching experience in Biochemistry and related courses. He obtained his Master's Degree in 2005. His research focuses on liposomal drug delivery nano systems,



NiO, ZnO, CuO, AgO, TiO, SnO, and WO have unlimited applications in the medical sector (drug delivery, cancer treatment, and tissue repair), environment (qualitative and quantitative analysis of pollutants and toxins, water purification, and photo-degradation), energy nanogenerators, electronics, catalysis, and mechanical and textile industries.<sup>11–17</sup>

Iron oxide is one of the best biocompatible inorganic nanoparticles, and it has remarkable microscopic physical properties including superparamagnetism, low susceptibility to oxidation, firmness in liquid solution, extended blood half-life, and flexible surface chemistry.<sup>18–22</sup> Also, from an application

point view, iron oxide NPs have high sustainability and superior properties in comparison to natural substances such as enzymes, which have drawbacks including high cost of isolation and purification, limited thermostability, and small pH window, which disrupts the enzyme activity upon handling, storage, and transportation.<sup>23,24</sup>

Artificial enzymes have replaced real enzymes in many applications for decades due to their stability and low cost. Metal complexes, cyclodextrins, polymers, dendrimers, and biomolecules have been studied to replicate enzyme activities and structures. Due to the rapid advancement of nano-studies and



Rana Said

*Dr Rana Said is an Associate Professor at Al-Ahliyya Amman University. She is specialist in sample preparation methods for the measurement of drugs and metabolites in biological samples to provide information that plays an important role in toxicokinetic and pharmacokinetic studies, and in therapeutic drug monitoring (TDM). She was always curious about drugs and how they work in the human body. She loved her chemistry*

*and biological classes at school given that they were related to understanding more about drugs. She worked at a pharmaceutical company for a short time, and she travelled to the UK to attend a Master's Pharmaceutical Program, and at the end, she did her research project at one of the biggest pharmaceutical companies in the UK, AstraZeneca. Subsequently, she left for Sweden and joined a pharmacology department to get a PhD in developing new drugs analysis methods for pharmacokinetic studies. It was not easy to do this considering that this university is ranked number 4 in the world and a lot of work was required.*



Obada A. Sibai

*Obada Sibai, a Syrian national, earned his BSc in Pharmacy from Al-Ahliyya Amman University, 2022. He is a Research Assistant in the Faculty of Pharmacy/Al Ahliyya Amman University. He is currently a Master's student in Pharmaceutical Sciences in the Faculty of Pharmacy/Al-Zaytoonah University. His current work is in drug discovery, especially in computational drug design. He has published five articles in*

*prestigious journals. He has excellent experience in many chemical synthesis and modelling software.*



Aseel AbuRuman

*Aseel Aburumman, a dedicated educator and pharmaceutical scientist, earned her Master's in Pharmaceutical Sciences in 2020 from Al-Ahliyya Amman University, Jordan. As a Lecturer at the same university, she imparts knowledge in different pharmaceutical aspects. Adept in research, her Master's project, "Development and In Vitro Evaluation of Soluplus® and/or Carbopol® 971 Buccoadhesive Patches Releasing Atorvastatin",*

*showcased her expertise in drug delivery. Aseel explored innovative approaches, including developing antipsychotic drugs with cancer treatment properties, demonstrating her commitment to advancing pharmaceutical science.*



Alaa S. Shraim

*Dr Ala'a S. Shraim holds the position of Assistant Professor at the Faculty of Allied Medical Sciences, Al-Ahliyya Amman University in Jordan. She has experience in the field of aptamer technology, namely, in the development and characterization of aptamers targeting kinases. She has developed her knowledge via extensive involvement in research, assessment, and teaching in academic institutions.*



the exceptional properties of nanomaterials, several nanomaterials have shown enzyme-like functions. Moreover, nanozymes are popular because of their ease of manufacture, storage, isolation, and exceptional outcomes. In this respect, IONzymes can be used effectively to mimic natural enzymes and applied in several environmental applications, such as degradation of antibiotics and adsorption of dyes, in the food industry and biomedical, biosensing, cosmetics, and bioengineering.<sup>25–32</sup>

In this review, we highlight the methods for the synthesis of IONzymes and the current advances in the development of their applications. We discuss several nanomaterials that have been studied to imitate various types of enzymes in order to highlight the advancement in the area of nanomaterial-based artificial enzymes. We discuss their synthetic methods, processes, and applications in several domains, such as biosensing and immunoassays, as well as pollution elimination. We also outline techniques, such as several green, chemical, and physical methods, to produce iron oxide nanozymes.

## 2. Synthesis approaches of IONzymes

The methods commonly used to produce metal oxide nanoparticles are often applied in the creation of IONzymes, especially when they consist primarily of two magnetic nanoparticles, namely, magnetite ( $\text{Fe}_3\text{O}_4$ ) and maghemite ( $\gamma\text{-Fe}_2\text{O}_3$ ).<sup>33</sup>

The synthesis of IONzymes is accomplished using different chemical, physical, and biological techniques. Co-precipitation, evaporative decomposition of solution (EDS), aerosol, ultrasonic, sol-gel synthesis, micro-emulsion methods, reverse micelles, flow injection, solid-state reaction, spraying, and hydrothermal/solvothermal processes are typically used in chemical synthesis.<sup>34</sup> The physical methods include milling, grinding, pyrolysis, and thermal ablation, as illustrated in



Afnan Al hunaiti

*Dr Afnan Al-Hunaiti, an Associate Professor at the University of Jordan, is a seasoned academic with a comprehensive background in chemistry and catalysis. She earned her PhD from the University of Helsinki in 2015, focusing on the oxidation of fine chemicals through iron-based and metal-free catalysis. With over a decade of experience, Dr Afnan has held positions at the University of Petra and conducted research at the University of*

*Helsinki. Dr Afnan's dedication extends to impactful publications in peer-reviewed journals, showcasing her commitment to advancing scientific knowledge in fields such as environmental inorganic chemistry and atmospheric catalysis. As an Associate Professor, Dr Afnan's multifaceted contributions underscore her significant role in advancing the understanding in the fields of catalysis and environmental science, making her a respected figure in the academic community.*

Fig. 1. Also, the “Green Approach” has recently attracted significant consideration due to its eco-friendly nature and sustainability, which can be conducted using algae, bacteria, fungi, and plants.

It is critical to distinguish between the general synthesis of iron oxide nanoparticles and specific processes that provide the characteristics of an enzyme in the production of IONzymes. Several conventional methods are effective in generating iron oxide nanoparticles, including co-precipitation, thermal breakdown, and hydrothermal synthesis. These steps must be performed to expose the properties of nanozymes. For instance, surface functionalization is essential to provide the ability to use enzymes.

Gao *et al.* (2007) demonstrated that the peroxidase-like activity of iron oxide nanoparticles can be significantly increased by adding specific functional groups to their surface. Both the size and structure of nanoparticles play a key role in determining their enzymatic activity.<sup>35</sup> Another study demonstrated that an increase in the surface area to volume ratio of smaller iron oxide nanoparticles leads to higher catalytic efficacy. This characteristic resembles the active regions of natural enzymes.<sup>36</sup> In addition, the crystalline structure of IONzymes influences their catalytic activity. Wei and co-workers showed that the intrinsic catalase-like, oxidase, and peroxidase activities of magnetite ( $\text{Fe}_3\text{O}_4$ ) nanoparticles are attributed to their spinel structure.<sup>37</sup>

The synthesis method influences the stability and specificity of IONzymes prior to catalytic activity. Research in a related study indicated that the value of adding stabilizing chemicals during the synthesis of IONzymes can improve the lifespan of their catalytic activity and their thermal stability.<sup>38</sup> This study emphasized that the functional characteristics of nanozymes are stable with time, stressing the importance of stabilization in the synthesis process.

Additionally, the effectiveness and selectivity of nanozymes can be altered by doping them with different metals towards particular substrates, hence expanding their applicative potential, as demonstrated by Zhang *et al.*<sup>39</sup> These features demonstrate the significance of carefully choosing the methods for the synthesis of IONzymes to induce enzymatic activity and particle formation. This approach is consistent with the principles of biomimetic design given that it features both the functional and physical attributes of the nanoparticles. This illustrates the intricate nature of enzymes found in biological systems.

### 2.1. Chemical synthesis

The chemical production of nanoparticles is the most typical technique. However, the key challenges in this type of procedure include particle dispersion, clumping, and size uniformity. Additionally, chemical-based procedures involve the use of solvents such potassium bitartrate, sodium dodecyl sulfate, sodium borohydride, and hydrazine, all of which are detrimental to the environment given that they produce unpleasant waste flows. Herein, we focus on the four most popular methods, as listed in Table 1.



**2.1.1. Co-precipitation.** Massart developed a chemical co-precipitation approach for the large-scale synthesis of hydrophilic IONzymes.<sup>44</sup> This reaction is performed in aqueous solution; therefore, the product is water-dispersed and may be directly employed for diverse applications without complicated ligand exchange procedures. The co-precipitation procedure to manufacture Fe<sub>3</sub>O<sub>4</sub> involves the hydrolysis and condensation of ferrous and ferric ions in aqueous solution in the pH range of 8–14, as shown in eqn (1).<sup>18</sup>



Co-precipitation relies on the pH, reaction temperature, ion concentration, ionic strength, salt type, and alkali used. However, the application of co-precipitation to create magnetite NPs is a challenging process, and the reaction conditions must be tightly regulated.<sup>45,46</sup>

Another factor is the molar ratio of ferrous/ferric, which affects the physical and magnetic properties of NPs. When 1 ferrous : 1 ferric is used, there is larger magnetization saturation than other ratios.<sup>47,48</sup> Similar research has been conducted to

create various synthesis techniques employing the chemical co-precipitation process to produce stable, homogeneous, smaller-sized, crystalline particles.<sup>49</sup>

A method involving co-precipitation in flow chemistry, combined with an *in situ* synchrotron X-ray diffraction (XRD) technique, was devised to “freeze” the transient reaction states through steady-state operation. This technique showed appealing findings, as follows:

(i) Five seconds after mixing, the only crystalline phase was the inverse spinel framework of magnetite/maghemite.

(ii) The particle size increased slightly, and solid phase development (owing to particle growth) was completed within 2 min.

(iii) The mixing conditions did not affect the XRD pattern.

(iv) During co-precipitation, the diffraction peaks widened, indicating the presence of smaller coherently scattered regions (Fig. 2).<sup>50,51</sup>

The co-precipitation chemical technique can be used to produce functional materials, as shown in Table 2. Chen *et al.* discovered a new co-precipitation approach to generate ferumoxytol, a therapeutically relevant magnetic nanoparticle with



Fig. 1 Chemical and physical techniques for the synthesis of IONzymes.



**Table 1** The most common chemical techniques employed for the synthesis of IONzymes

| Synthetic technique           | Advantage   | Disadvantage  | Ref. |
|-------------------------------|---|---|------|
| Co-precipitation              | Water-dispersed<br>Environmentally friendly<br>Efficient and economical   | Multi-variable dependence<br>Toxic liquid waste<br>Requires trained person for maintenance and regeneration<br>Toxic liquid waste | 40   |
| Hydrothermal/<br>solvothermal | Simple procedure<br>Rapid particle formation<br>Producing highly crystalline nanocrystals<br>Well-controlled dimensions<br>Combined with microwaves and magnetic fields improves reproducibility and quality  | High temperature and pressure range<br>Anti-corrosion autoclave material<br>Relatively costly reactors                            | 41   |
| Electrochemical<br>deposition | Short formation time<br>Simple apparatus<br>Uniformly coated on complicated geometries<br>Control of film thickness and morphology  | Mass production is not possible<br>Stable solvent media<br>High electrophoretic mobility  | 42   |
| Sol-gel synthesis             | Simplicity of the process<br>Uniform composition and high purity<br>High production efficiency<br>Production of intricately shaped optical components<br>Controlling homogeneous products<br>Capacity to use the product with unique structures such as fibers and aerogels | Wear resistance reduced<br>Weak bonding strength<br>Hard to regulate porosity and permeability                                    | 43   |

$\gamma$ -Fe<sub>2</sub>O<sub>3</sub> as the core. The magnetization of ferumoxytol is the greatest recorded to date, reaching 104–105 emu g<sup>-1</sup>, and its crystal structure has been substantially improved.<sup>52</sup> Superparamagnetic IONzymes were produced with a limited size distribution, and their magnetic susceptibility, coercivity, remanence, and saturation magnetization at 5–300 K were analyzed.<sup>53</sup>

**2.1.2. Hydrothermal and solvothermal.** The technique employed for the synthesis of IONzymes can alter the primary properties of the generated IONzymes. The solvothermal and hydrothermal processes are the most effective chemical ways to

create nanomaterials, specifically nanocrystals with precise dimension control.<sup>55</sup> The suggested process begins with the formation of nuclei from the solute molecules, which subsequently undergo significant growth during heating, leading to the formation of the final crystal structure (Fig. 3). The reaction rate increases together with crystallinity.<sup>56</sup> Highly crystalline iron oxide nanoparticles with a size in the range of 14 and 25 nm were produced in a pressure-resistant reactor at 473 K.<sup>57</sup> However, this method requires costly reactors.<sup>58</sup>

Many advances have contributed to a deeper understanding and improved this technique (Table 3). A novel strategy was

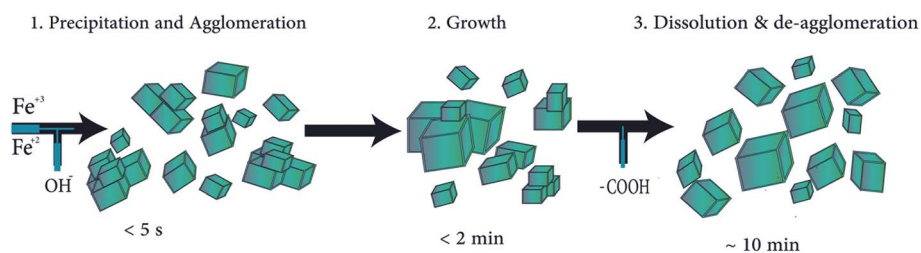


**Fig. 2** Suggested particle mechanism during the co-precipitation procedure: (1) particles are precipitated and agglomerated within 5 s, (2) agglomerated pieces grow over the next 2 or 3 min and (3) addition of neutralization solution causes particles to de-agglomerate within 10 min.

**Table 2** Representative iron oxides obtained through co-precipitation procedures

| Compound/property               | Particle size (nm) | Morphology | Magnetization (emu g <sup>-1</sup> ) | Ref. |
|---------------------------------|--------------------|------------|--------------------------------------|------|
| Ferumoxytol                     | 7.1                | Spherical  | 104–105                              | 52   |
| Temperature-dependent particles | 11.22              | Spherical  | 64–72                                | 53   |
| (Zn–Mn)-co-doped                | 10–13              | Spherical  | 81                                   | 54   |



demonstrated to control the carbon chain length of the iron(III) carboxylate precursors and the amount of reaction solvent in the solvothermal synthesis of FeO nanocrystals.<sup>59</sup> Additionally, deep eutectic solvents with hydrated mixtures have been applied to solvothermal approaches for the preparation of functional nanomaterials.<sup>51</sup> A study presented the first *in situ* and static structural analysis of the production of iron oxide (hematite) nanoparticles in a deep eutectic solvent (DES) of choline chloride : urea.<sup>60</sup> González-Rivera *et al.* created a quick and easy approach. By directly applying microwave radiation in the solvothermal reactor with the aid of a coaxial antenna, the synthesis was thermally initiated, accelerated, and controlled. This method was perfectly regulated in short synthesis periods utilizing the phosphorylated nanoreactor.<sup>61</sup>

**2.1.3. Electrochemical deposition.** The electrophoretic deposition (EPD) technique involves the use of charged particles that move and are deposited on the surface of a conductive electrode to create thin or thick coatings and films. A broad range of fine powder, composite particles, colloidal metals, and ceramics can be produced *via* EPD.<sup>64</sup> EPD is one of several solution methods employing colloidal NPs, which has recently emerged as a successful method for producing dense and durable NP films. The relationship in EPD systems between

colloidal NPs and the organic solvent has been studied using hexane, toluene, and chloroform in various solvent ratios to examine the charge formation function of the solvent in EPD systems (10 : 0, 7 : 3, 5 : 5, 3 : 7, and 0 : 10). The NP layer gets thicker and rougher as the toluene to hexane ratio increases. Alternatively, the film thickness is dramatically reduced when the chloroform to hexane ratio increases.<sup>65</sup>

The electrophoretic deposition approach was used to produce a bioactive coating, such as hydroxyapatite-iron oxide-chitosan (HA-CS) with varying amounts of Fe<sub>3</sub>O<sub>4</sub> (1, 3, and 5 wt%) and porous morphology.<sup>13</sup> Another methodology demonstrated potential for generating thick magnetic nanocomposites for on-chip power components by incorporating iron oxide nanoparticles into a mold, and subsequently performing electro-infiltration of nickel through the porous film. The resulting magnetic saturation of the nanocomposites was measured at 473 kA m<sup>-1</sup>, which is intermediate between the magnetic saturation values of iron oxide nanoparticles and nickel.<sup>66</sup> Also, the formulated and cost-effective coating method can enhance the surface characteristics and hemocompatibility for biomedical applications, resulting in decreased contact angle values and hydrophilic nature. In one study, the Ti-13Nb-13Zr alloy was electrophoretically coated with Bioglass (BG),



Fig. 3 Schematic representation of crystal growth mechanisms under hydrothermal/solvothermal conditions.

Table 3 Representative iron oxide nanozymes obtained through advanced hydrothermal/solvothermal procedures

| Variable/technique                           | Starting materials   | Solvent                                      | Particle size (nm)            | Morphology      | Ref.      |
|--|--|--|-------------------------------|-----------------|-----------|
| Deep eutectic-solvothermal                   | Iron(III) nitrate nonahydrate  | 1 : 2 : 10 choline chloride : urea : water   | 5–9                           | Oblate spheroid | 51 and 60 |
| Size-controlled facile solvothermal method   | FeCl <sub>3</sub> · 6H <sub>2</sub> O NaAc polyvinyl pyrrolidone (PVP) | Ethylene glycol (EG) diethylene glycol (DEG) | 23                            | Spherical       | 33        |
| Ligands and solvent composition              | FeCl <sub>3</sub> · 6H <sub>2</sub> O sodium carboxylate               | 2 : 1 water : ethanol                        | 25                            | Cubic           | 59        |
| Oxidation-precipitation solvothermal process | FeCl <sub>2</sub> · 4H <sub>2</sub> O                                  | Deionized water                              | 33                            | Spherical       | 62        |
| Microwave solvothermal treatment             | FeCl <sub>3</sub> · 6H <sub>2</sub> O sodium citrate                   | Ethylene glycol (EG)                         |                               | Irregular       | 63        |
| Magnetothermally-responsive nanocarriers     | FeCl <sub>2</sub> · 4H <sub>2</sub> O                                  | Ethylene glycol (EG) urea                    | 50 nm diameter, 250 nm length | Tubular shape   | 61        |



hydroxyapatite (HA), and iron oxide particles (FeO), which improved the stability of the suspension.<sup>67</sup>

**2.1.4. Sol-gel synthesis.** Using the sol-gel method, a gel-like network is generated, incorporating both liquid and solid phases. Also, by selecting the appropriate complexing agent, concentration, type of chemical additives, and temperature settings, it is possible to control the crystallinity, shape, and magnetic characteristics of IONzymes.<sup>68,69</sup> Apparently, the annealing temperature plays a central role in this method, and the outcome shows that the crystalline Fe<sub>2</sub>O<sub>3</sub> nanoparticles<sup>70</sup> and the dielectric properties are enhanced.<sup>71</sup> Additionally, this technique can be used to create products with efficient physical characteristics, such as low UV absorption and thermal expansion coefficient and high optical transparency.<sup>72</sup>

The crystalline structure, composition, purity, magnetism, and morphology of iron oxide nanomaterials can be enhanced by optimizing some variables or combining techniques (Table 4). One technique is optimizing the precursor-to-solvent (P/S) ratio for three iron oxide phases ( $\alpha$ -Fe<sub>2</sub>O<sub>3</sub>, Fe<sub>3</sub>O<sub>4</sub>, and  $\gamma$ -Fe<sub>2</sub>O<sub>3</sub>) to tune the structural and magnetic properties *via* sol-gel synthesis.<sup>73</sup> Another method combines microwave radiation and aluminum doping in iron oxide thin films, which controls the structural transitions of the iron oxide thin film. A study demonstrated a  $\gamma$ -Fe<sub>2</sub>O<sub>3</sub> to Fe<sub>3</sub>O<sub>4</sub> transition at 6–10 wt% Al with increasing saturation magnetization of the films from 251.3 emu cm<sup>-3</sup> to 405.6 emu cm<sup>-3</sup>.<sup>74</sup>

## 2.2. Physical genesis

Physical techniques such as mechanical milling, grinding, and thermal ablation are all expensive given that they consume a significant amount of energy. Furthermore, another significant drawback of this strategy is its exceedingly low output yield.

**2.2.1. Ball milling.** Ball milling is a shear-force-dominated method, which is also known as mechanical alloying, ultra-fine grinding, and nanosizing in the literature. It is one of the most widely used industrial processes, in which the particle size

is continuously reduced by impact and attrition. Metal balls, often made of zirconia (ZrO<sub>2</sub>) or steel, serve as the grinding medium, while a spinning shell generates centrifugal force. By regulating the milling variables, such as ball-to-powder ratio (B/P), milling time, milling rpm, starting weight, and ball diameter, the excessive compression force that may harm the crystalline characteristics of nanomaterials can be reduced. Table 5 demonstrates examples of two states of milling that can be initiated, *i.e.*, dry ball milling (DBM) and wet ball milling (WBM). The solid-state mechanical size reduction process known as ball milling transforms iron precursors into MNPs (magnetic nanoparticles). To speed up milling and prevent the agglomeration of the created nanoparticles, solvents or excess salt can be added.<sup>78</sup>

Also, different mechanical ball milling techniques can be applied, such as conventional ball milling. Specifically, larger particles collide with steel balls or the interior wall of the tank to produce ultrafine particles, while high-energy ball milling uses a specialized grinding machine to synthesize a nano-spinel-type ferrite by mechanically alloying the initial materials.<sup>79</sup> However, the significant drawbacks of ball milling are pollution of the steel ball, the potential chemical and mechanical amorphization of the crystals, the high power used, and the prolonged milling period.<sup>79,80</sup>

**2.2.2. Electron beam lithography.** The use of electron beam lithography or electron beam deposition to apply either an exposure-sensitive resist material or high-purity iron material to a substrate can be employed for the synthesis of MNPs. This process produces MNPs by evaporating the first iron precursors onto the resist pattern, and then removing the resist through a lift-off procedure. Alternatively, the nanopatterns can be etched onto a functional substrate to produce MNPs.<sup>78,84</sup>

**2.2.3. Laser ablation.** Laser ablation is a method that involves irradiating a solid material placed under a thin layer with a laser beam.<sup>80,85</sup> When the solid material is placed at the bottom of a cell containing a liquid,<sup>86</sup> the technique is referred

Table 4 Representative iron oxide nanozymes obtained through sol-gel procedures

| Variable/technique   | Starting materials  | Solvent                                   | Particle size (nm) | Morphology   | Additional property             | Ref. |
|----------------------|---|---|--------------------|--|---------------------------------|------|
| Agitation time       | Fe (NO <sub>3</sub> ) <sub>3</sub> ·9H <sub>2</sub> O<br>Ba (NO <sub>3</sub> ) <sub>2</sub> | Absolute ethanol                          | 10 nm              | Spherically  | Purity > 75%                    | 75   |
| Carbonization method | FeCl <sub>3</sub> ·6H <sub>2</sub> O/<br>rosin  | Deoxygenated H <sub>2</sub> O/<br>ethanol | <50 nm             | Varies with different rosins:<br>FeCl <sub>3</sub> | Enhances interfacial reactivity | 76   |
| Non-hydrolytic       | Anhydrous<br>FeCl <sub>3</sub>  | Anhydrous ethanol                         | 202–373 Å          | Rod-shaped   | Homogeneous dispersion          | 77   |

Table 5 Iron oxide-based nanomaterials prepared *via* ball milling process

| Milling process | Equipment/ball properties       | Milling agent/solvents and conditions | Characteristics   | Ref. |
|-----------------|---------------------------------|---------------------------------------|---|------|
| WBM             | Planetary ball mill             | DI water, 4 h, 500 rpm                | High adsorption capacities of Cr(IV) $q_e = 48.1 \text{ mg g}^{-1}$ | 34   |
| DBM             | Iron balls with 1.5 cm diameter | 30 h and 90 h                         | 31.48 emu g <sup>-1</sup> and 37.80 emu g <sup>-1</sup>             | 81   |
| DBM             | Steel balls with 8 mm diameter  | 25 rpm, 60 min                        | Particle size = 45 nm   | 82   |
| DBM             | Planetary ball mill             | 30 min, 320 rpm                       | $M_s = 20.45 \text{ emu g}^{-1}$                                    | 83   |



to as “laser ablation synthesis in solution (LASiS)”. In this case, various lasers can be employed, including Nd:YAG, Ti:sapphire, and copper vapor lasers,<sup>80,87</sup> allowing precise control of the phase composition, size, and shape of the particles, thus producing nanoparticles with an average diameter of approximately 15 nm.<sup>87</sup> Although laser ablation can quickly generate MNPs when exposed to a laser for short periods, this method has a low production rate.<sup>88</sup> Also, prolonged laser ablation leads to the formation of an excessive number of nanoparticles, which remain suspended in the colloidal solution and obstruct the laser beam. This causes the laser energy to be absorbed by the previously formed nanoparticles, rather than the target surface, resulting in a decreased ablation rate.<sup>80</sup>

**2.2.4. Sputtering.** Sputtering is a process that entails bombarding the surface of a bulk material with high-energy particles, such as noble gas ion beams, to remove atoms from the surface. This method produces nanoparticles with the same composition as the target material and is more cost-effective than electron beam lithography.<sup>80</sup> However, the choice of sputtering gas, such as helium, neon, argon, krypton, and xenon, can impact the surface morphology, texture, and optical properties of the resulting nanoparticles.<sup>89,90</sup>

**2.2.5. Aerosol spray pyrolysis.** Aerosol spray pyrolysis is a scalable and cost-effective physical synthesis process.<sup>91</sup> In this method, nanoparticle precursors are transmitted into a heated reactor in the form of small droplets suspended in a vapor, obtaining MNPs with a spherical morphology, narrow particle size distribution, and no agglomeration.<sup>80</sup> However, there are still challenges to be addressed, such as difficulty in controlling the homogeneous pore sizes and inner structure of the particles.<sup>91,92</sup>

Spray pyrolysis is a chemical vapor deposition (CVD) process used to prepare nanomaterials, which have a consistent particle diameter compared to the traditional nanomaterials.<sup>93,94</sup> A precursor solution of metallic salts is used to create an aerosol in the spray pyrolysis process. The produced solution droplets (aerosol) undergo several stages, as follows: (1) solvent evaporation from the droplet surfaces, (2) drying, (3) annealing, (4) production of microporous particles with a defined phase structure, (5) creation of solid particles, and (6) sintering of

solid parts. Fig. 4 shows these steps starting from precursors to nanozyme formation.<sup>95</sup>

Several studies were conducted to investigate the influence of different substrate temperatures,<sup>96,97</sup> sampling techniques,<sup>98</sup> presence of chloride ion,<sup>99</sup> and other dispersion parameters<sup>100</sup> on the pyrolysis process. Interestingly, highly porous ternary NiCoFe oxide nanomesh with a two-dimensional shape and quasi-single-crystalline (QSC) property was created using a practical molten-salt-protected pyrolysis method.

The NiCoFe oxide nanomesh possessed high stability, low over-potential, high current density, and excellent oxygen evolution reaction performance with increased intrinsic activity. A quick pyrolysis technique shielded by molten salt (MS, 53% KNO<sub>3</sub>, 7% NaNO<sub>3</sub>, and 40% NaNO<sub>2</sub>) was carried out at 300 °C to produce mild dehydration to form mixed metal oxides with retained morphology and minimum particle sintering.<sup>101</sup> Another study employed the phase-selective laser-induced breakdown spectroscopy technique to investigate the production of FeO particles along the axial centerline of the spray in an external mixing spray flame pyrolysis reactor, under different precursor solutions. The addition of 2-ethylhexanoic acid to the precursors was examined and significant changes in the evolution of the atomic emission spectra were observed. These changes enabled the differentiation between the gas-to-particle and droplet-to-particle routes *in situ*.<sup>102</sup>

### 2.3. Biosynthesis

Green synthesis, which involves the use of plants, microbes, and other biological materials, has gained significant attention as a safe, sustainable, and biologically acceptable method for the synthesis of metal oxide nanoparticles, such as iron oxide nanoparticles (IONPs) (Fig. 5). IONPs have attracted particular interest due to their magnetic properties, which allow them to be easily separated from the reaction mixture using an external magnetic field. Biomaterials such as plants, fungi, bacteria, and algae can be used in green synthesis to produce IONPs with a size in the range of 1 to 100 nm and a variety of shapes, including cubic, tetragonal crystalline, spherical, cylindrical, elliptical, octahedral, orthorhombic, hexagonal rods, nanospheres, and quasi spherical. In addition to synthesizing IONPs,

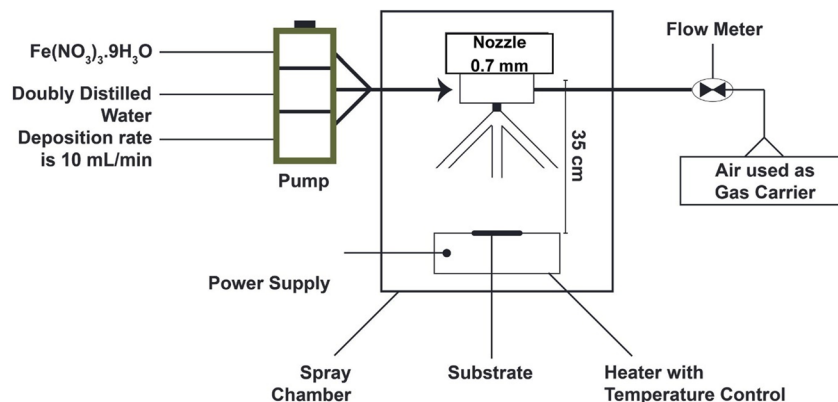


Fig. 4 Setup of the spray pyrolysis technique used for synthesis IONzymes thin film at various temperatures.





Fig. 5 Biosynthesis of IONzymes using different green sources.

these biomaterials can also act as reducing agents, capping agents, stabilizing agents, and fabricating agents in the green synthesis of nanoparticles.<sup>103</sup>

It is important to highlight the diverse biological pathways employed by various organisms. For instance, *Plumeria obtusa* leaves were employed for the biofabrication of well-defined, crystalline INPs *via* an eco-friendly, cost-effective, and surfactant-free technique. These nanoscale particles displayed potent antimicrobial and antioxidant activity, while remaining non-toxic to red blood cells. This green synthesis presented a potential strategy for the synthesis of sustainable nanomedicines against microbial infections.<sup>104</sup> A study revealed the eco-friendly biosynthesis of IONPs from *Penicillium* spp. fungal filtrate. The extracellular strategy starts by the reduction of  $\text{FeCl}_3$ , with the protein from *Penicillium* spp. playing a pivotal role in capping and stabilizing the IONPs. The characterization of the IONPs showed that they were spherical with high stability. The IONPs exhibited powerful antibacterial and antioxidant activities, making them potential alternatives to antimicrobial and anticancer agents in biomedical applications.<sup>105</sup>

A notable example is the use of bacterial extracellular polymeric substances (EPS) as reducing and stabilizing compounds during the bio-mediated production of metal nanoparticles for multifunctional applications, such as a new bacterium, *E. faecalis*\_RMSN6. The EPS was extracted from *E. faecalis* and used for producing highly stable IONPs. This study aimed to assess the effectiveness of the synthesized  $\text{Fe}_3\text{O}_4$  NPs as adsorbents for removing  $\text{Cr}(\text{VI})$  metal ions from aqueous solutions. Furthermore, an *in vitro* toxicity analysis using bacterial EPS was conducted to evaluate the potential adverse effects of the synthesized  $\text{Fe}_3\text{O}_4$  NPs.<sup>106</sup>

Shalaby *et al.* presented a green synthesis method for the preparation of recyclable IONPs utilizing *Spirulina platensis* microalgae. This study highlighted the efficient adsorptive

removal of cationic and anionic dyes for water treatment applications. The environmentally friendly synthesis method not only contributes to the sustainable formation of nanomaterials but also exhibits the recyclability of the synthesized IONPs.<sup>107</sup>

**2.3.1 Biosynthesis of IONPs using plants.** Plants are widely available, easy to handle, and relatively inexpensive materials that can be used for the synthesis of various types of nanoparticles.<sup>108</sup> Different parts of plants, such as their roots, leaves, seeds, flowers, fruits, peels, petals, and whole plants, can be utilized in the biosynthesis process because they contain various biomolecules, such as amino acids, carbohydrates, terpenoids, flavonoids, saponins, proteins, and nitrogenous compounds, which can act as reducing agents, stabilizers, redox mediators, and capping agents in the synthesis of nanoparticles<sup>109–116</sup> (Table 6).

**2.3.2 Biosynthesis of IONPs using fungi.** The synthesis of iron oxide nanoparticles using fungal species has several advantages, including ease of scaling up the process, use of economical raw materials for growth, high biomass-forming capacity of fungi, simplicity of the downstream processing steps, low toxicity of the residue, and economic feasibility of the process.<sup>180–182</sup> Fungal species also have superior tolerance and bioaccumulation properties, which can aid in the synthesis of metal nanoparticles.<sup>93</sup> The relationship between microorganisms and metals has been thoroughly researched and applied in various biological processes, including bioleaching, heavy metal removal, and bioremediation.<sup>183</sup> In these processes, microorganisms can accumulate and extract metals through the release of enzymes or other mechanisms. These interactions have practical applications in fields such as biotechnology, environmental science, and metallurgy (Table 7).<sup>116,184</sup>

**2.3.3 Biosynthesis of IONPs using bacteria.** Prokaryotes, which are simple organisms without a defined nucleus or



Table 6 Biosynthesis of iron oxide nanoparticles using plants

| Name of the plant               | Biomaterial used             | Iron precursor used  | Size                | Shape                                | Application   | Ref. |
|---------------------------------|------------------------------|--|---------------------|--------------------------------------|---|------|
| <i>Hibiscus rosa-sinensis</i>   | Dried petals                 | Ferric chloride (25 mM) and ferrous chloride (25 mM) (2 : 1)   | 65 nm               | Spinel                               | Biscuit fortification   | 117  |
| <i>Carica papaya</i>            | Dried leaves                 | FeCl <sub>3</sub> ·6H <sub>2</sub> O (0.1 M), NaOH (1 M)   | 2.159 nm            | Not uniform (agglomerated particles) | Antibacterial   | 118  |
| <i>Psidium guajava</i>          | Leaves                       | FeCl <sub>3</sub> ·6H <sub>2</sub> O   | 1–5 nm              | Spherical                            | Antibacterial   | 119  |
| Citrus                          | Fresh leaves                 | Iron chloride (0.1 mM)   | 15–80 nm            | Spherical                            | Antibacterial   | 120  |
| <i>Malus pumila</i> (apple)     | Peels                        | FeCl <sub>2</sub> ·4H <sub>2</sub> O (20 mM), FeCl <sub>3</sub> ·6 H <sub>2</sub> O (40 mM), NaOH (1 M)                                | 50–100 nm           | Elliptical and spherical             | Decolorization of dye   | 121  |
| <i>Citrus paradisi</i>          | Peels                        | FeCl <sub>3</sub> ·6H <sub>2</sub> O (6 mM)  | 28–32 nm            | Spherical                            | Antioxidant   | 122  |
| <i>Syzygium cumini</i>          | Leaves                       | FeCl <sub>3</sub> (0.010 mol L <sup>-1</sup> )   | 40–52 nm            | Spherical                            | Antibacterial, antifungal, aflatoxin B1 adsorption  | 123  |
| <i>Juglans regia</i>            | Dried green husk             | FeCl <sub>3</sub> ·6H <sub>2</sub> O (97%), FeCl <sub>2</sub> ·4H <sub>2</sub> O (99%), NaOH (2 M)                                     | 12.6 nm             | Cubic                                | Cytotoxic assay   | 124  |
| <i>Pyrus sinkiangensis</i> Yu   | Peels                        | FeSO <sub>4</sub> ·7H <sub>2</sub> O (0.1 M)   | 10–90 nm            | Irregularly shaped                   | Cr(IV) removal  | 125  |
| <i>Cymbopogon citratus</i>      | Leaves                       | FeCl <sub>3</sub> ·6H <sub>2</sub> O (0.26 M), FeCl <sub>3</sub> ·6H <sub>2</sub> O (0.52 M), Na <sub>2</sub> CO <sub>3</sub> (0.75 M) | 9 ± 4 nm            | Irregular cubic                      | Nanotoxicological   | 126  |
| <i>Laurus nobilis</i>           | Leaves                       | FeCl <sub>3</sub> ·6H <sub>2</sub> O (0.1 M)   | 8.03 ± 8.99 nm      | Spherical                            | Antimicrobial   | 127  |
| <i>Hyphaene thebaica</i>        | Fruits                       | FeH <sub>12</sub> N <sub>2</sub> O <sub>12</sub> (5 g)   | 5–10 nm             | Quasi-spherical and cuboidal         | Antimicrobial, antioxidant, and antiviral   | 128  |
| <i>Solanum lycopersicum</i>     | Leaves                       | FeSO <sub>4</sub> ·5H <sub>2</sub> O (0.1 M)   | 200–800 nm          | Flower                               | Antibacterial and anticancer  | 129  |
| <i>Lawsonia inermis</i>         | Leaves                       | FeSO <sub>4</sub> (0.01 M)   | 2 μm                | Hexagonal                            | Antimicrobial   | 130  |
| <i>Ficus carica</i>             | Fruit                        | (F <sub>2</sub> Cl <sub>3</sub> ·6H <sub>2</sub> O) (100 mL)   | 11–29 nm            | Spherical                            | Antimicrobial   | 131  |
| <i>Rhamnus Triquetra</i>        | Leaves                       | Ferric acetate (3 g)   | ~21 nm              | Spherical                            | Antimicrobial, antioxidant, anticancer, antileishmanial, brine shrimp cytotoxicity        | 132  |
| <i>Trigonella foenumgraecum</i> | Leaves                       | FeCl <sub>3</sub> (1 M)  | 27.91–40.94 nm      | Grain                                | Antibacterial   | 133  |
| Tomato                          | Fruits                       | FeCl <sub>3</sub> (1 M)  | 48.18–77.54 nm      | Semispherical                        | Antibacterial   | 133  |
| Grapes                          | Fruits                       | FeCl <sub>3</sub> (16.2 g)   | 49–50 nm            | Cubic                                | Antibacterial   | 134  |
| <i>Moringa oleifera</i>         | Leaves                       | FeCl <sub>3</sub> (0.5 M)  | 15.01 ± 6.03 nm     | Rod-like                             | Antibacterial   | 135  |
| <i>Withania coagulans</i>       | Berries                      | FeCl <sub>3</sub> ·6H <sub>2</sub> O, FeCl <sub>2</sub> ·4H <sub>2</sub> O (1 : 2 M)   | 16 ± 2–18 ± 2 nm    | Rods                                 | Photocatalytic degradation and antimicrobial  | 136  |
| <i>Citrullus colocynth</i>      | Pulp<br>Seed                 | FeCl <sub>3</sub> (0.5 M)  | 12–45 nm<br>6–15 nm | Spherical                            | Antimicrobial   | 137  |
| <i>Durian rind</i>              | Peels                        | Ferrous sulfate (0.05 M)   | 10 nm               | Spherical                            | Antibacterial   | 138  |
| <i>Borassus flabellifer</i>     | Seed coat                    | Ferric chloride (0.2 M), ferrous sulphate (0.1 M) (2 : 1)  | 30–200 nm           | Hexagonal                            | Antimicrobial, antioxidant  | 139  |
| <i>Citrus sinensis</i>          | Peels                        | Ferric chloride (1 mM)   | 97.5 nm             | —                                    | Antibacterial   | 140  |
| <i>Thymbra spicata</i>          | Leaves                       | FeSO <sub>4</sub> ·7H <sub>2</sub> O (0.1 M)   | 120.3–1793.9 nm     | Spherical                            | Antibacterial, antibiofilm, and antioxidant   | 141  |
| <i>Cocos nucifera</i> L.        | Pulps                        | 0.502 g of FeCl <sub>3</sub>   | 90–95 nm            | Husked rice shape                    | Antibacterial and anticancer  | 142  |
| <i>Euphorbia herita</i>         | Leaves                       | Ferrous sulfate (0.1 M), ferric chloride (0.1 M)   | 25–80 nm            | Cavity like                          | Antimicrobial   | 143  |
| <i>Camellia sinensis</i> L      | Grinded waste of pruned teas | FeSO <sub>4</sub> ·5H <sub>2</sub> O (0.1 M), NaOH (0.5 M)   | 28.5 nm             | Regular spherical                    | Antioxidant   | 144  |
| <i>Gundelia tournefortii</i> L  | Leaves                       | FeCl <sub>3</sub> ·6H <sub>2</sub> O (2 M), FeSO <sub>4</sub> ·7H <sub>2</sub> O (1 M), NaOH (1 M)                                     | 29.9 nm             | Spherical                            | Remove crystal violet, malachite green, and safranin dyes from prepared aqueous solutions | 145  |



Table 6 (Contd.)

| Name of the plant  | Biomaterial used | Iron precursor used   | Size             | Shape                          | Application  | Ref. |
|--|------------------|---|------------------|--------------------------------|--|------|
| <i>Aegle marmelos</i>  | Leaves           | Ferric nitrate (90 mL)  | —                | Agglomerated                   | Antimicrobial and antifungal   | 146  |
| <i>Alstonia scholaris</i>                                    | Leaves           | FeCl <sub>2</sub> ·4H <sub>2</sub> O (0.5 M)<br>MgCl <sub>2</sub> ·6H <sub>2</sub> O (0.5 M)            | 8.14–13.4 nm     | Cubic                          | Antimicrobial, antioxidant and larvicidal  | 147  |
| <i>Polyalthia longifolia</i>                                 | Leaves           | FeCl <sub>2</sub> ·4H <sub>2</sub> O (0.5 M)<br>MgCl <sub>2</sub> ·6H <sub>2</sub> O (0.5 M)            | 8.14–13.4 nm     | Cubic                          | Antimicrobial, antioxidant and larvicidal  | 147  |
| Coffee   | Seed             | Fe <sup>2+</sup> and Fe <sup>3+</sup> (1 : 1)   | 23.2–37.5 nm     | Cubic                          | Antibacterial  | 148  |
| <i>Brassica oleracea</i> var. <i>Capitata sub.var. rubra</i> | Peels            | Iron(III) chloride (10 mM)  | 675 ± 25 nm      | Agglomerated                   | Anticancer   | 149  |
| <i>Zingiber officinale</i>                                   | Root             | Ferric chloride (0.1 M)   | 5.10 nm          | Nanocube                       | Antimicrobial  | 150  |
| <i>Artemisia</i>   | Leaves           | FeCl <sub>3</sub> (0.01, 0.04, 0.07, and 0.1 M)   | 24.67–34.28 nm   | Cubical                        | Antioxidant  | 151  |
| <i>Garcinia mangostana</i>                                   | Peels            | FeCl <sub>3</sub> ·6H <sub>2</sub> O and FeCl <sub>2</sub> ·4H <sub>2</sub> O at a molar ratio of 2 : 1 | 13.42 ± 1.58 nm  | Spherical                      | Anticancer   | 152  |
| <i>Chlorophytum comosum</i>                                  | Leaves           | FeCl <sub>3</sub> ·6H <sub>2</sub> O (0.1 M)  | <100 nm          | Spherical                      | Methyl orange dye degradation and antimicrobial                                      | 153  |
| <i>Mikania mikrantha</i>                                     | Leaves           | FeSO <sub>4</sub> ·7H <sub>2</sub> O (5 mmol) and FeCl <sub>3</sub> (10 mmol)                           | 20.27 nm         | Rhomboidal                     | Antimicrobial  | 154  |
| Garlic   | Peels            | FeCl <sub>3</sub> (1 M)   | 24–44 nm         | Irregular                      | Degrade methylene blue dye   | 155  |
| Onion  | Peels            | FeCl <sub>3</sub> (1 M)   | 29–32 nm         | Nanofiber                      | Degrade methylene blue dye   | 155  |
| <i>Ficus carica</i>  | Leaves           | FeCl <sub>3</sub> ·6H <sub>2</sub> O (0.01 M), NaOH (0.1 M)   | 43–57 nm         | Agglomerated and are multiform | Antioxidant  | 156  |
| <i>Celosia argentea</i>                                      | Leaves           | Ferric nitrate (0.1 M)  | 5–10 nm          | Spherical                      | Antibiofilm, antioxidant, anti-inflammatory, antidiabetic, and larvicidal activities | 157  |
| <i>Plumeria obtusa</i>                                       | Leaves           | Fe(C <sub>2</sub> H <sub>3</sub> O <sub>2</sub> ) <sub>2</sub> (3 mM)                                   | 50 nm            | Spheroidal                     | Antimicrobial, antioxidant   | 104  |
| <i>Camellia sinensis</i>                                     | Leaves           | FeCl <sub>3</sub> (10 mM)   | 13 nm            | Cubical                        | Antioxidant, antimicrobial   | 158  |
| <i>Persimmon</i>   | Fruits           | FeCl <sub>3</sub> (0.04 M), NaOH (1 M)  | 30–60 nm         | Spherical                      | Antibacterial and anticancer   | 159  |
| <i>Punica granatum</i>                                       | Peels            | FeCl <sub>3</sub> (0.1 M)   | 17.8 ± 6.5 nm    | Cubical                        | Enzyme mimicking peroxidase, catalase, and superoxide dismutase                      | 160  |
| <i>Buddleja lindleyana</i>                                   | Leaves           | Fe (SO <sub>4</sub> ) <sub>3</sub> ·6H <sub>2</sub> O (1 g), AgNO <sub>3</sub> (0.1 g)                  | 25 and 174 nm    | Triangular and spheroidal      | Antimicrobial  | 161  |
| <i>Hibiscus rosa sinensis</i>                                | Flowers          | FeCl <sub>2</sub> ·4H <sub>2</sub> O (1 mM)   | 51 nm            | Tetragonal                     | Antibacterial  | 162  |
| <i>Allium cepa</i>   | Peel             | Ferric chloride (250 mL)  | 42.78 1 nm       | —                              | Memory-enhancing agent   | 163  |
| <i>Centaurea alba</i>  | Leaves           | FeCl <sub>3</sub> ·H <sub>2</sub> O (0.001 M)   | 10–52 nm         | Spherical                      | Anti-atherosclerotic and antioxidant   | 164  |
| <i>Peltophorum pterocarpum</i>                               | Leaves           | FeSO <sub>4</sub> ·7H <sub>2</sub> O (0.1 M)  | 0.085 to 0.2 μm  | Irregular                      | Photocatalytic and catalytic removal of organic pollutants                           | 165  |
| <i>Psidium guajava</i> Linn                                  | Leaves           | FeCl <sub>3</sub> (1 M), NaOH (1 N)   | 80.3–99.1 nm     | Spherical                      | Antimicrobial, antioxidant   | 166  |
| <i>Hylocereus undantus</i>                                   | Fruits           | Ferric sulphate and ferrous sulphate (2 : 1)  | 10–15 nm         | Spherical                      | —  | 167  |
| <i>Nigella sativa</i>  | Seeds            | FeCl <sub>3</sub> (1 M) and FeCl <sub>2</sub> (2 M)   | 31.45 nm         | Spherical                      | Antimicrobial  | 168  |
| <i>Mentha spicata</i>  | Leaves           | FeCl <sub>3</sub> (0.4 M)   | 21–82 nm         | Circular or rod                | Antimicrobial  | 169  |
| <i>Cassia auriculata</i>                                     | Flowers          | FeCl <sub>3</sub> ·6H <sub>2</sub> O (0.1 M)  | 15–35 nm         | Spherical                      | Photocatalytic degradation and larvicidal effect                                     | 170  |
| <i>Melia azedarach</i>                                       | Flowers          | Ferrous sulphate (20 mM), NaOH (0.1 M)  | 231.43 ± 5.21 nm | Spherical                      | Antimicrobial, antioxidant   | 171  |
| <i>Echinochloa frumentacea</i>                               | Grains           | Fe(NO <sub>3</sub> ) (0.1 M)  | 20–40 nm         | Rectangular and triangular     | Pharmaceutical, agricultural, targeted drug delivery and biomedical applications     | 172  |
| <i>Pimenta dioica</i>  | Leaves           | FeSO <sub>4</sub> (0.1 M)   | 5–15 nm          | Spherical                      | Anticancer   | 173  |



Table 6 (Contd.)

| Name of the plant             | Biomaterial used | Iron precursor used   | Size           | Shape                  | Application   | Ref. |
|-------------------------------|------------------|---|----------------|------------------------|---|------|
| <i>Banana</i>                 | Peels            | FeCl <sub>3</sub> ·6H <sub>2</sub> O (2.16 g)<br>CH <sub>3</sub> COONa (6.56 g)                               | 44–58 nm       | Cubic and agglomerated | Nondestructive technique (NDT) applications               | 174  |
| <i>Amla</i>                   | Seeds            | FeCl <sub>3</sub> (0.01 M)  | 4–5 nm         | Spherical              | Removal of toxic dyes                                     | 175  |
| <i>Centaurea solstitialis</i> | Leaves           | FeCl <sub>3</sub> (0.1 M)   | —              | Spherical              | Antimicrobial activity and dye decolorization             | 176  |
| <i>Eucalyptus globulus</i>    | Leaves           | Fe(NO <sub>3</sub> ) <sub>3</sub> ·9H <sub>2</sub> O (0.1 M)  | 2.34 ± 0.53 nm | Spherical              | Removal of heavy metals from agricultural soil            | 177  |
| <i>Galega officinalis</i>     | Leaves           | FeCl <sub>3</sub> ·6H <sub>2</sub> O (40 mM),<br>FeCl <sub>2</sub> ·4H <sub>2</sub> O (20 mM) (2 : 1 M ratio) | 41.9 ± 1.00 nm | Spherical              | Toxicity assessment in plants and aquatic model organisms | 178  |
| <i>Coriandrum sativum</i> L.  | Leaves           | FeSO <sub>4</sub> (0.01 mM)   | 163.5 nm       | Spherical              | —   | 179  |

membrane-bound organelles, have been extensively studied as a model system in the field of nanotechnology due to their widespread presence, fast doubling time, ability to grow under challenging conditions, and the fact that they can be cultivated using inexpensive and straightforward media.<sup>191,192</sup> The

application of this system is considered an effective method for synthesizing nanoparticles with a range of shapes, sizes, structural frameworks, and physical and chemical properties through the reduction of metal ions using reductase enzymes, which allow microorganisms to accumulate and detoxify

Table 7 Biosynthesis of iron oxide nanoparticles using fungi

| Fungal strain                   | Biomaterial used   | Iron precursor used  | Size (nm)      | Shape           | Applications                            | Ref. |
|---------------------------------|--------------------|--|----------------|-----------------|---|------|
| <i>Aspergillus niger</i> BSC-1  | Cell-free filtrate | (FeCl <sub>3</sub> ·6H <sub>2</sub> O) and ferrous sulfate (FeSO <sub>4</sub> ·7H <sub>2</sub> O) in 2 mM:1 mM | 20–40 nm       | Orthorhombic    | Cr(vi) removal                          | 182  |
| <i>Penicillium</i> spp.         | Cell-free filtrate | FeCl <sub>3</sub> (3 mM)   | 3.31–10.69 nm  | Spherical       | Antimicrobial, antioxidant              | 105  |
| <i>Chaetomium cupreum</i>       | Fungal biomass     | FeSO <sub>4</sub> (2 g) and NaOH (1.20 g)  | 25 nm          | Spherical       | Anticancer                              | 185  |
| <i>Chitosan</i>                 | —                  | (FeCl <sub>3</sub> ·6H <sub>2</sub> O), (FeSO <sub>4</sub> ·4H <sub>2</sub> O)                                 | 200–600 nm     | Spherical       | Postharvest disease inhibition in fruit | 186  |
| <i>Penicillium roqueforti</i>   | Fungal biomass     | Ferric chloride hexahydrate (10 <sup>-3</sup> M) and ferrous chloride tetrahydrate (10 <sup>-3</sup> M)        | 5–16 nm        | Spherical       | Antimicrobial                           | 187  |
| <i>Lichen Ramalina sinensis</i> | —                  | Fe <sup>2+</sup> /Fe <sup>3+</sup> (100 mL)  | 31.74–53.91 nm | Spherical       | Antimicrobial                           | 188  |
| <i>Pleurotus florida</i>        | —                  | Ferric chloride (1 M)  | 100 nm         | Spherical       | Antimicrobial                           | 189  |
| <i>Penicillium commune</i>      | —                  | FeCl <sub>3</sub> (1 mM), FeSO <sub>4</sub> (1 mM)   | 30–50 nm       | Spherical       | Cleaning gel                            | 190  |
| <i>Bacillus megaterium</i>      | —                  | FeCl <sub>3</sub> (1 mM), FeSO <sub>4</sub> (1 mM)   | 40–60 nm       | Cubic           | Cleaning gel                            | 190  |
| <i>Fusarium oxysporum</i>       | —                  | FeCl <sub>3</sub> (1 mM), FeSO <sub>4</sub> (1 mM)   | 20–50 nm       | Quasi-spherical | Cleaning gel                            | 190  |

Table 8 Biosynthesis of iron oxide nanoparticles using bacteria

| Bacteria                     | Salt   | Size           | Shape                                    | Applications                      | Ref. |
|------------------------------|--|----------------|--|-----------------------------------|------|
| <i>Bacillus subtilis</i>     | FeCl <sub>3</sub> (2 mM)   | 12–32 nm       | Spherical                                | Cytotoxicity assay                | 196  |
| <i>Bacillus subtilis</i>     | FeCl <sub>3</sub> (2 mM)   | 3.6 nm         | Spherical                                | —                                 | 196  |
| <i>Proteus vulgaris</i>      | FeCl <sub>3</sub> (3 mM)   | 20–30 nm       | Spherical                                | Antibacterial, antioxidant        | 197  |
| <i>Enterococcus faecalis</i> | FeCl <sub>2</sub> ·4H <sub>2</sub> O (0.1 M), FeCl <sub>3</sub> ·6H <sub>2</sub> O (0.2 M) | 15.4 nm        | Cubical, hexagonal, brick, and irregular | Heavy metal removal and cytotoxic | 106  |
| <i>Enterococcus faecalis</i> | FeCl <sub>2</sub> ·6H <sub>2</sub> O (1 M)   | 48.77–55.55 nm | Cubic                                    | Antibiofilm                       | 198  |
| <i>Bacillus coagulans</i>    | FeCl <sub>3</sub> ·6H <sub>2</sub> O, FeCl <sub>2</sub> ·4H <sub>2</sub> O (2 : 1 M)       | 15.18 nm       | Cubic                                    | Antibacterial                     | 199  |
| <i>Aeromonas hydrophila</i>  | FeCl <sub>2</sub> (5 mmol), FeCl <sub>3</sub> hexahydrate (10 mmol)                        | 8–12 nm        | Spherical                                | Antibacterial                     | 200  |



Table 9 Biosynthesis of iron oxide nanoparticles using algae

| Algae  | Biomaterial used          | Iron precursor salt   | Size                      | Shape                          | Applications  | Ref. |
|--|---------------------------|---|---------------------------|--------------------------------|---|------|
| <i>Spirulina platensis</i>                       | Powder                    | FeCl <sub>3</sub> ·6H <sub>2</sub> O (from 0.1 to 0.6 M)                                      | <10 nm                    | Slightly irregular and rounded | Adsorptive removal of cationic and anionic dyes             | 107  |
| <i>Sargassum vulgare</i> ( <i>Phaeophyceae</i> ) | Powder                    | FeCl <sub>3</sub> (0.1 M)   | 22.73 nm                  | Nanospheres                    | Antibiofilm   | 204  |
| <i>Ulva fasciata</i> ( <i>Chlorophyceae</i> )    | Powder                    | FeCl <sub>3</sub> (0.1 M)   | 28.41 nm                  | Nanospheres                    | Antibiofilm   | 204  |
| <i>Jania rubens</i> ( <i>Rhodophyceae</i> )      | Powder                    | FeCl <sub>3</sub> (0.1 M)   | 27.78 nm                  | Nanospheres                    | Antibiofilm   | 204  |
| <i>Sargassum crassifolium</i>                    | Dried powder              | (FeCl <sub>3</sub> : FeCl <sub>2</sub> ) (0.1 : 0.05 and 0.02 : 0.01)                         | 40–215 nm                 | Quasi-spherical                | —   | 205  |
| <i>Chlorella vulgaris</i>                        | Powder                    | FeSO <sub>4</sub> ·7H <sub>2</sub> O and Fe(NO <sub>3</sub> ) <sub>3</sub> ·9H <sub>2</sub> O | 4.855, 5.702 and 3.614 nm | Amorphous biochar              | Adsorbent for dye removal                                   | 206  |
| <i>Aegagropila linnaei</i>                       | Powder                    | FeSO <sub>4</sub> ·7H <sub>2</sub> O (0.01 mol)   | 100–150 nm                | Geomorphic                     | Adsorption and Fenton-like reaction                         | 207  |
| <i>Ulva lactuca</i>                              | Powder                    | FeCl <sub>3</sub> ·6H <sub>2</sub> O (28 mM), FeSO <sub>4</sub> ·7H <sub>2</sub> O (14 mM)    | 50–80 nm                  | Spherical                      | Adsorptive removal of Pb(II) from heavy metal bearing water | 208  |
| <i>Ulva prolifera</i>                            | Dried-refrigerated powder | FeSO <sub>4</sub> ·7H <sub>2</sub> O (0.1 M)  | 41.23 nm                  | Spherical                      | As(III) removal   | 209  |

metals.<sup>193</sup> This process involves the use of metal salts as precursors in the reaction and has been used to synthesize metallic nanoparticles.<sup>116,194,195</sup> Table 8 presents some types of bacteria used to produce IONzymes.

**2.3.4 Biosynthesis of IONPs using algae.** Algae, which include both microalgae (single-celled organisms) and macroalgae or seaweeds (multi-celled organisms), are used in the field of nanotechnology for the synthesis of various types of metallic nanoparticles, such as gold, silver, palladium, iron, and copper (Table 9).<sup>201,202</sup> Similar to plants and bacteria, algae also produce a range of biomolecules, including proteins, fats, carbohydrates, peptides, alkaloids, terpenes, macrolides, cell wall polysaccharides, glycoproteins (containing functional groups such as carbonyl, hydroxyl, carboxyl, and sulfonate), and enzymes, which play a key role in the reduction, capping, fabrication, and stabilization of nanoparticles.<sup>201–203</sup> The use of algae in the production of nanoparticles is considered a safe, simple, cost-effective, and environmentally friendly approach.<sup>116</sup>

### 3. Structure and design

Functionalized polymeric MNPs exhibit certain distinguished features for drug delivery in terms of effectiveness and efficiency compared to traditional oral and intravenous techniques. This is because they can control the particle size, morphology, and surface charge,<sup>210–212</sup> which enhance the drug delivery and release by joining with other molecules such as antibodies, proteins, and ligands. This can help reduce the side effects associated with chemotherapy, radiotherapy, and surgery.<sup>213</sup> MNPs used for biomedical purposes are often composed of metals such as iron and iron oxide, which can possess a variety of morphologies.

Iron oxide MNPs with nanocrystalline magnetite (Fe<sub>3</sub>O<sub>4</sub>) cores are preferred for biomedical applications because of their

biocompatibility (they swiftly decompose into non-toxic iron and oxygen elements *in vivo*), biodegradability,<sup>214–216</sup> and ease of manufacturing.<sup>135,217</sup> Iron oxide nanoparticles (FeO-NPs) are classified into two categories, *i.e.*, superparamagnetic iron oxide nanoparticles (SPIONs) and ultra-small superparamagnetic iron oxide nanoparticles (USPIONs). These two classes have different relaxometry properties and mean hydrodynamic sizes.<sup>214</sup> SPIONs are made of iron oxide cores with average diameters in the range of 3–20 nm and composed of agglomerates with a hydrodynamic diameter of more than 50 nm.<sup>214</sup> Therefore, any spherical FeO-NPs with a diameter equal to or less than 20 nm will exhibit SPION behavior, which can be used to facilitate targeted drug delivery in the treatment of oncological diseases (Fig. 6).

Magnetite has a face-centered cubic (FCC), closed packing cubic, and inverse spinel structure with the ferric (Fe<sup>3+</sup>) ion occupying all the tetrahedral (T<sub>h</sub>) sites and both ferric (Fe<sup>3+</sup>) and ferrous (Fe<sup>2+</sup>) ions occupying the octahedral (O<sub>h</sub>) sites. It has attracted significant attention due to the hopping of electrons between Fe<sup>2+</sup> and Fe<sup>3+</sup> ions in its octahedral lattice at ambient temperature, as well as its low toxicity (Fig. 6). This is because the iron oxide core of magnetite degrades to low molecular weight iron, making it a useful material in biomedical applications and an effective carrier for drug delivery to target locations, avoiding the negative effects of oral and intravenous drug delivery.<sup>218–227</sup> This is due to the unique properties of magnetite, such as its biocompatibility, lack of toxicity, targeting ability, biodegradability, chemical stability, stable dispersion, and magnetic stability.<sup>228–232</sup>

Due to the anisotropic dipolar attraction and high surface energies of FeO-NPs, large surface-to-volume ratio unmodified FeO-NPs tend to form clusters of large aggregates, which can reduce their surface area to volume ratio and decrease their effectiveness. Additionally, FeO-NPs are prone to oxidation in air, which can lead to the loss of magnetization because of their chemical activity from the oxidation of ferrous (Fe<sup>2+</sup>) to ferric



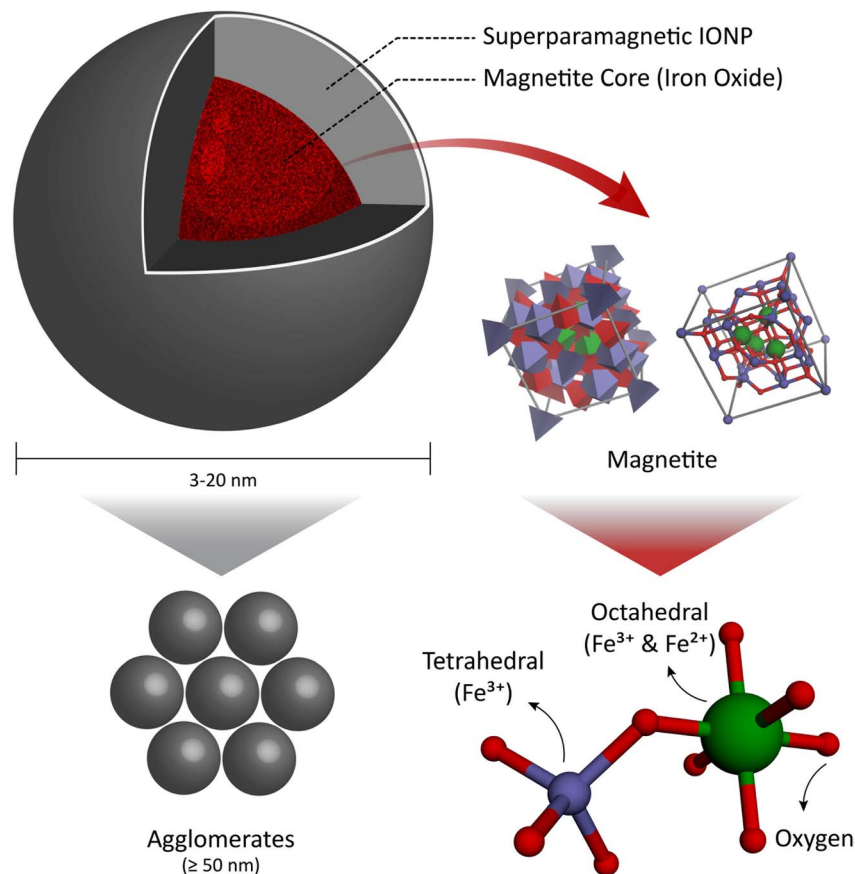


Fig. 6 (a) Superparamagnetic iron oxide nanoparticles (SPIONs). (b) Face-centered cubic (FCC) closed packing, with  $\text{Fe}^{3+}$  in the tetrahedral sites and  $\text{Fe}^{2+}$  occupying the octahedral sites.

( $\text{Fe}^{3+}$ ) ions. Thus, to avoid this oxidation, experiments with FeO-NPs are often conducted under dry conditions.<sup>232–234</sup>

## 4. Characteristics and applications of IONzymes

Nanomaterials have established numerous novel applications to improve human health, ranging from diagnosis to therapeutic effects, control, and monitoring environment pollution, together with improving the chemical industry.<sup>235–237</sup> Iron oxide nanomaterials have versatile applications that are not limited to their magnetic properties. IONzymes are considered one of the most representative nanozymes being explored for their kinetics and catalytic properties.<sup>238</sup> IONzymes have several benefits in real applications, particularly in biomedicine. In this section (Fig. 7), we focus on the biomedical and environmental applications of IONzymes.

### 4.1. Characteristics of IONzymes

Recently, diverse nanomaterials with enzyme-like actions were discovered with catalytic properties such as the natural oxidoreductase enzyme family as artificial enzymes or enzyme mimics.<sup>239–243</sup> Recently, researchers have utilized IONzymes in numerous innovative biomedical applications due to their

enzyme-like activities.<sup>244–246</sup> In addition, the features of IONzymes are not limited to catalytic activity, where they are also widely applied as biosensors, biomarkers, and in immunoassay approaches.<sup>247–249</sup> Here, we intend to highlight the importance of IONzymes in biomedical applications.

**4.1.1. Enzymatic-like characteristics.** In 2007, it was reported for the first time that iron oxide nanomaterials display enzymatic-like characteristics. Gao *et al.* stated that FeO-NPs showed basic peroxidase (POD)-like activity, with catalytic behavior similar to horseradish POD (HRP).<sup>250</sup> Since then, IONzymes and their typical POD and catalase (CAT)-like activities have attracted attention because they have been proven to work under physiological conditions like natural enzymes, including the same substrate, pH, and temperature. Moreover, they follow similar kinetics and pathways as conventional enzymes.<sup>251–255</sup> IONzymes are stated to mimic the peroxidase and catalase enzymes. Both enzymes have a porphyrin heme as a cofactor in their active site and utilize hydrogen peroxide as the substrate. Also, both enzymes play a crucial role in avoiding cellular oxidative damage in aerobically respiring creatures by forming free radicals and oxygen.<sup>240,256,257</sup>

**4.1.1.1. IONzymes mimic POD activity.** POD-like activity was verified for both  $\text{Fe}_2\text{O}_3$  and  $\text{Fe}_3\text{O}_4$  IONzymes, which catalyzed a colorimetric reaction including hydrogen peroxide ( $\text{H}_2\text{O}_2$ ) utilizing the same optimal conditions as HRP at the





Fig. 7 Applications of IONzymes.

physiological temperature and in acidic media.<sup>258</sup> In addition, IONzymes can function over several substrates, including 3,3',5,5'-tetramethylbenzidine (TMB), *o*-phenylenediamine (OPD), 3,3'-diaminobenzidine (DAB), 2,2'-azino-bis(3-ethylbenzthiazoline-6-sulfonic acid) (ABTS),<sup>250,259,260</sup> polydopamine,<sup>261</sup> terephthalic acid (TA),<sup>262</sup> luminol, and benzoic acid.<sup>263</sup> Moreover, IONzymes could peroxidize biomolecules such as proteins, nucleic acids, sugars,<sup>264</sup> and lipids.<sup>265</sup>

Furthermore, the enzymatic activity of IONzymes similar to natural PODs can be affected by several natural effectors. ATP, ADP, AMP,<sup>265–267</sup> and DNA are the main activators to improve the POD-like activity of IONzymes by involving them in the electron transfer mechanism.<sup>268,269</sup> Free radical quenchers as sodium azide, ascorbic acid, hypotaurine, and catecholamines were found to decrease the POD activity of IONzymes<sup>270,271</sup> by delaying the affinity of the substrate to IONzymes more than quenching the free radicals.<sup>238</sup>

**4.1.1.2. IONzymes mimic catalase activity.** IONzymes have been reported to exhibit catalase-like activity *via* H<sub>2</sub>O<sub>2</sub> decomposition under neutral and high pH conditions. As previously described for POD and proven by Chen *et al.*, pH plays a significant role in the effectiveness of the H<sub>2</sub>O<sub>2</sub> decomposition rate.<sup>259</sup>

**4.1.1.3. Kinetics of IONzymes.** IONzymes, as POD and CAT enzymes, follow Michaelis–Menten behavior.<sup>272</sup> The apparent affinity of a substrate to the enzyme (KM) value for H<sub>2</sub>O<sub>2</sub> was higher for IONzymes compared to the native HRP, indicating that IONzymes have a lower affinity to H<sub>2</sub>O<sub>2</sub> than HRP by nearly 41-fold.<sup>250</sup> Alternatively, the KM value for TMB against IONzymes was lower than that of HRP, indicating that the IONzymes have a higher affinity to TMB than the natural enzyme.<sup>273</sup> Given that IONzymes have an abundance of iron ions, this

increases their POD activity by around 40-times compared to HRP.<sup>250</sup>

The rate of the CAT activity depends on the O<sub>2</sub> production rate in the solution. IONzymes also adopt Michaelis–Menten kinetics for the CAT reaction.<sup>259</sup> The volumetric measurement of oxygen gas is influenced by many other parameters, such as temperature and O<sub>2</sub> diffusion and can be attained by a volumetric bar-chart chip.<sup>274</sup>

**4.1.1.4. Mechanism of action of IONzymes.** IONzymes show a catalytic mechanism similar to HRP, where they react with H<sub>2</sub>O<sub>2</sub> to form hydroxyl free radicals (<sup>•</sup>OH) as an intermediate state like the POD enzyme state. <sup>•</sup>OH captures H<sup>+</sup> from the hydrogen donor such as TMB.<sup>265</sup> Interestingly, the produced <sup>•</sup>OH does not have reaction specificity and can bind to any hydrogen donors, leading to a wide range of applications.<sup>275</sup>

During the activity of IONzymes, two types of free radicals are produced, *i.e.*, <sup>•</sup>OH and hydroperoxyl (HO<sub>2</sub><sup>•</sup>) radicals. The ferryl ion (FeO<sup>2+</sup>) that is typically formed in POD catalysis is not detected in the POD-like IONzyme activity but produced in the CAT-like IONzyme activity.<sup>276,277</sup> Moreover, IONzymes have two iron types, *i.e.*, Fe<sup>2+</sup> and Fe<sup>3+</sup>, where Fe<sup>2+</sup> ions may play a major role in their catalytic POD-like activity.<sup>250</sup>

The POD-like activity arises also from the integral nanoparticles rather than free iron ions, and thus the IONzyme mechanism performance includes kinetic procedures involving substrate binding, surface reaction, and product release, displaying similar enzymatic kinetics.<sup>278,279</sup> Furthermore, IONzymes can be utilized as an exceptional carrier to load other enzymatic functionalities on their surface. For example, glucose oxidase (GOx) can form a new nano-complex by GOx catalyzing glucose to produce hydrogen peroxide, which in turn can be catalyzed by IONzymes.<sup>280</sup>



## 4.2. Biomedical applications of IONzymes

**4.2.1. Immunoassay, diagnosis, therapy, and biomarker detection.** Based on the superiority of IONzymes over HRP, they can be used as an alternative to HRP in the enzyme-linked immunosorbent assay (ELISA) and other associated molecular detection procedures through the conjugation of antibodies.<sup>281,282</sup> Based on the superparamagnetism of IONzymes, they can be used to enhance antigen detection at low concentrations.<sup>283</sup> Gao *et al.* developed chitosan-modified magnetic nanoparticles (CS-MNPs) as additional enzymes in conventional ELISA configurations, with  $1 \text{ ng mL}^{-1}$  detection limit for a carcinoembryonic antigen (CEA).<sup>281</sup> Similar approaches were adapted to detect other antigens or pathogens, containing immunoglobulin G (IgG), hepatocellular carcinoma biomarker Golgi protein 73 (GP73),<sup>284</sup> human chorionic gonadotropin (HCG),<sup>285</sup> mycoplasma pneumonia,<sup>286</sup> *Vibrio cholerae*, rotavirus,<sup>287</sup> cancer cells with human epidermal growth factor receptor 2 (HER2),<sup>287,288</sup> and epidermal growth factor receptor (EGFR).<sup>289</sup> Daun *et al.* developed an iron oxide nanozyme-strip to sense Ebola virus (EBOV) with a detection limit as low as  $1 \text{ ng mL}^{-1}$  for EBOV glycoprotein.<sup>290</sup> Moreover, the surface of IONzymes was covered with streptavidin to attain signal amplification *via* IONzyme catalysis by Thiramanas *et al.* to sense *Vibrio cholerae* with a sensitivity of  $10^3 \text{ CFU mL}^{-1}$  in drinking and tap water.<sup>291</sup> Moreover, Zhang *et al.* established a colorimetric aptasensor for the determination of thrombin by employing chitosan-modified  $\text{Fe}_3\text{O}_4$  (MNPs). The results exhibited that the thrombin absorption values improved in a concentration-dependent manner with a linear range from 1 to 100 nM.<sup>292</sup> Based on the aptamer conjugated to the IONzymes,  $\text{Fe}_3\text{O}_4$  NPs with an aptamer-based immunosorbent assay (NAISA) were developed for aflatoxin B1 (AFB1) recognition with better operation and separation. The aptamer was implemented

to diagnose AFB1, and this method showed a limit of detection of  $5 \text{ pg mL}^{-1}$  (Fig. 8).<sup>293</sup>

Magnetoferritin NPs (M-HFn) are a certain type of IONzymes that are linked to the recombinant human heavy-chain ferritin (HFn) protein shell, which binds to transferrin receptor 1 (TfR1) overexpressed in most tumor cells.<sup>294</sup> This approach enables tumor diagnosis by utilizing the POD/CAT functionality of the  $\text{Fe}_3\text{O}_4$  core to yield a color reaction, which can be utilized to visualize cancer tissues. This strategy can differentiate cancerous cells from normal cells with a sensitivity of 98% and specificity of 95%.<sup>238,295</sup> IONzymes and their POD activity can be used in bio-distribution studies. Based on this technique, Zhuang reported that dextran-coated  $\text{Fe}_3\text{O}_4$  NPs were confined in the liver, spleen, and lungs more than the kidney, lymph nodes, and thymus (Fig. 9A).<sup>295</sup>

In addition, IONzymes showed a therapeutic effect on tumor cells and against bacterial growth by catalyzing  $\text{H}_2\text{O}_2$  to produce toxic radicals.<sup>296,297</sup> To increase the intracellular  $\text{H}_2\text{O}_2$  concentration,  $\text{H}_2\text{O}_2$  was directly injected, or an enzyme was merged to generate  $\text{H}_2\text{O}_2$ . The former showed a significant inhibition efficacy against a mouse model bearing subcutaneous HeLa tumors.<sup>296</sup> Ferumoxytol was utilized with a low concentration of  $\text{H}_2\text{O}_2$  to fight oral biofilms and avoid dental decay. Ferumoxytol, carboxymethyl dextran-coated IONzymes could catalyze the decomposition of  $\text{H}_2\text{O}_2$  to hydroxyl radicals (Fig. 9B).<sup>298</sup> However, due to the increased toxicity of the  $\text{H}_2\text{O}_2$  injection option, incorporating an  $\text{H}_2\text{O}_2$ -producing enzyme is considered an efficient and safer choice. For example, Huo *et al.* reported that  $\text{Fe}_3\text{O}_4$  NPs and GOx co-entrapped in mesoporous silica NPs could be used for tumor catalytic therapy.<sup>299</sup>

Moreover, iron-based NPs can cause generate sufficient reactive oxygen species (ROS) to induce apoptosis in tumor cells into (ferroptosis).<sup>300,301</sup> For example,  $\text{Fe}^{3+}$  is reduced to  $\text{Fe}^{2+}$  by the overexpressed glutathione (GSH) in tumor tissues, leading



Fig. 8 Schematic presentation of nanozyme and aptamer-based immunosorbent assay (NAISA): (A) preparation of m-SAP/cDNA and (B) construction of NAISA for AFB1 detection.



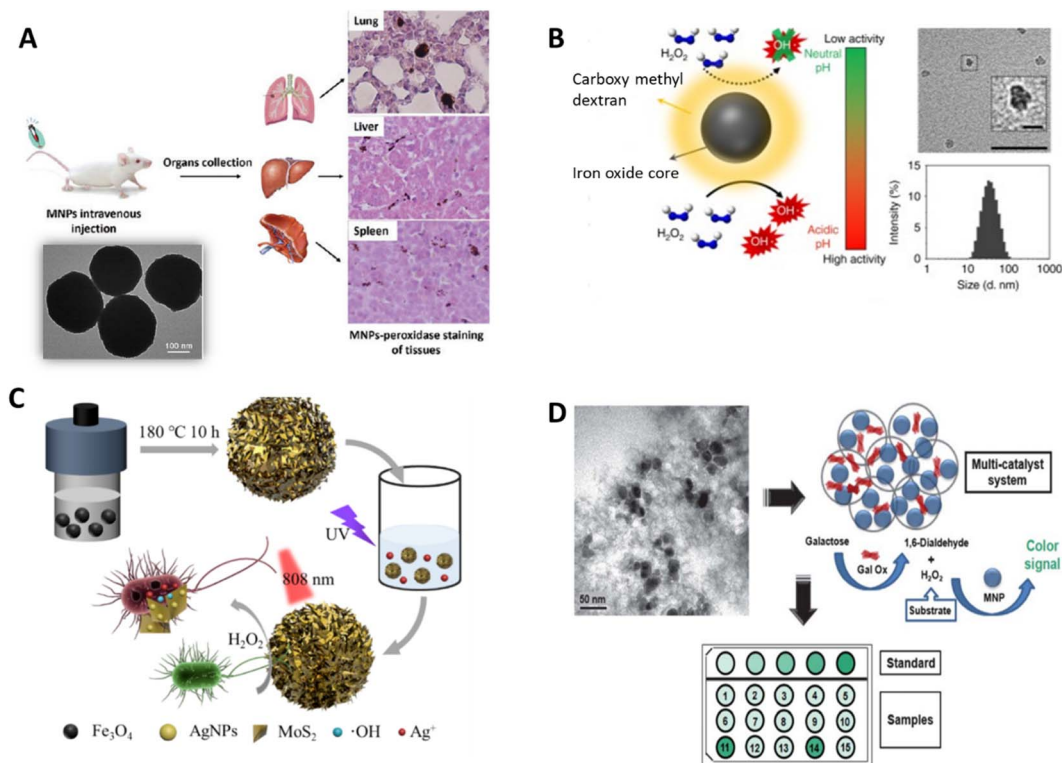


Fig. 9 Schematic illustration of (A) investigation of dextran-coated  $\text{Fe}_3\text{O}_4$  NPs in the liver, spleen, and lungs<sup>295</sup> and (B) pH-dependent catalytic activity of ferromoxytol. (Insets) negative stain TEM of ferromoxytol (Scale bar: 50 nm and 10 nm for close image) and hydrodynamic diameter measurements.<sup>298</sup> (C) Recoverable peroxidase-like  $\text{Fe}_3\text{O}_4@(\text{MoS}_2-\text{Ag})$  nanozyme with enhanced antibacterial ability.<sup>303</sup> (D) Multi-catalyst system for the quantification of galactose, entrapping both MNPs and Gal Ox in mesocellular silica.<sup>316</sup>

to the promotion of ROS production and resultant tumor ferroptosis.<sup>257,302</sup> In addition, Wei *et al.* developed  $\text{Fe}_3\text{O}_4@(\text{MoS}_2-\text{Ag})$  IONzymes that showed a good antibacterial effect against *E. coli* (~69.4%) by the generated ROS through POD-like activity and released  $\text{Ag}^+$  (Fig. 9C).<sup>303</sup> Furthermore, Wang *et al.* conveyed that a new cobalt-doped  $\text{Fe}_3\text{O}_4$  ( $\text{Co}@(\text{Fe}_3\text{O}_4)$ ) IONzyme exhibited better POD activity and a 100-fold higher affinity to  $\text{H}_2\text{O}_2$  than  $\text{Fe}_3\text{O}_4$  nanozymes to generate ROS for kidney tumor catalytic therapy *in vitro* and *in vivo*, presenting a potential novel avenue for tumor nanozyme catalytic treatment.<sup>304</sup> Similarly, Sun *et al.* improved highly toxic ROS levels from iron oxide core-shell mesoporous silica nanocarrier-mediated Fenton reactions for cancer therapy.<sup>305</sup> Furthermore, Li *et al.* prepared an  $\text{H}_2\text{O}_2$ -responsive POD and CAT-mimic  $\text{PtFe}@(\text{Fe}_3\text{O}_4)$  IONzyme, which displaced a 99.8% anti-tumor rate for deep pancreatic cancer in collaboration with photothermal treatment.<sup>306</sup> In a recent study, the application of adenosine triphosphate disodium salt (ATP) as a synergistic agent increased the generation of OH radicals and restored the antibacterial activity of  $\text{Fe}_3\text{O}_4$  IONzymes over the full pH range against both Gram-positive (*B. subtilis*) and Gram-negative (*E. coli*) bacterial strains in the presence of  $\text{H}_2\text{O}_2$  at a pH of around 7.0.<sup>307</sup>

**4.2.2. Enzyme-IONzyme nanoassembly.** This approach utilizes IONzymes loaded with oxidase enzymes to enable the fast colorimetric detection of biomolecules. The natural enzyme usually produces  $\text{H}_2\text{O}_2$  as an intermediate, which is catalyzed by the activity of the POD like-IONzymes.<sup>308</sup>

Glucose oxidase is the main enzyme assembled with IONzymes for the detection of glucose.<sup>309,310</sup> Firstly, GOx catalyzes glucose to produce  $\text{H}_2\text{O}_2$ , which is then catalyzed by IONzymes, and a color signal can be formed related to the amount of glucose with a detection limit of 0.5 to 3  $\mu\text{M}$ .<sup>311-314</sup> Other oxidases and esterases can also be utilized in this approach such as cholesterol oxidase for cholesterol detection,<sup>315,316</sup> galactose oxidase (Gal Ox) for galactose (Fig. 9D),<sup>316</sup> alcohol oxidase (AIOx) for alcohol,<sup>317</sup> and acetylcholine esterase (AChE) for acetylcholine (ACh).<sup>265</sup>

**4.2.3. Biosensors.** Several IONzymes have been used by researchers for the development of IONzyme-based biosensors for biomedical applications. IONzyme-based biosensors are based on the mimicking activity of IONzymes and can be categorized into three main groups: POD, oxidase, and CAT mimics.<sup>318</sup> Table 10 summarizes the reported IONzyme-based biosensors together with their enzyme-simulating activities and sensing mechanism.

#### 4.3. Environmental applications of IONzymes

Due to their high catalytic activity, stability, and multifunctionality, IONzymes have shown an increasingly wide range of applications in the biomedical, agricultural, and environmental fields.<sup>329-331</sup> Given that IONzymes possess intrinsic POD and CAT properties and follow a Fenton and/or Haber-Weiss reaction mechanism (including  $\cdot\text{OH}/\text{HO}_2\cdot$ ), they can be utilized



Table 10 IONzyme-based biosensors and their type of enzyme-mimicking activities and sensing procedures

| IONzymes  | Enzyme-mimicking activities | Biotarget                                   | Biosensor type                         | Ref. |
|---|-----------------------------|---|--|------|
| Fe <sub>3</sub> O <sub>4</sub>                  | POD                         | Ebola virus                                 | Colorimetric                           | 319  |
| Fe <sub>3</sub> O <sub>4</sub> -Pt/core-shell   | POD                         | Human chorionic gonadotropin (hCG)          | Colorimetric (paper-based strip)       | 320  |
| Fe-MOF-Au NPs                                   | POD                         | <i>Salmonella enteritidis</i>               | Colorimetric immunosensor              | 321  |
| Fe <sub>3</sub> O <sub>4</sub>                  | POD                         | Glucose                                     | Colorimetric                           | 322  |
| Fe <sub>3</sub> O <sub>4</sub>                  | POD                         | <i>Listeria monocytogenes</i>               | Colorimetric                           | 323  |
| Fe <sub>3</sub> O <sub>4</sub>                  | POD                         | Prostate-specific antigen                   | Photoelectrochemical (PEC) immunoassay | 324  |
| Fe <sub>3</sub> O <sub>4</sub>                  | POD                         | Micro RNA                                   | Electrochemical                        | 325  |
| Fe <sub>3</sub> O <sub>4</sub>                  | POD                         | Hepatitis B virus surface antigen (preS1)   | Colorimetric, immunoassay              | 250  |
| Fe@PCN-224 NPs                                  | POD                         | Glucose                                     | Colorimetric                           | 326  |
| Fe <sub>3</sub> O <sub>4</sub> @C               | POD                         | Platelet-derived growth factor BB (PDGF-BB) | Colorimetric                           | 327  |
| Fe <sub>3</sub> O <sub>4</sub> /CoFe-LDH hybrid | POD                         | Ascorbic acid                               | Colorimetric                           | 328  |

for the degradation of organic pollutants by combining free radical production with the magnetic characteristics of iron oxide.<sup>332</sup> Moreover, the catalytic activity IONzymes can be used for environmental monitoring, for example, detecting H<sub>2</sub>O<sub>2</sub> in rainwater and measuring heavy metals in environmental samples. The environmental applications of IONzymes are considered suitable for numerous environmental conditions, relatively easy and cheap, and can be simply applied to the screening of pesticides, organophosphorus compounds, and other ingredients. IONzymes can determine pollutants indirectly when they enable a target to undergo an alteration in chemical properties and react with the colorimetric sensor to be detected.<sup>333</sup>

A histidine-modified Fe<sub>3</sub>O<sub>4</sub> IONzyme offered an easy, inexpensive approach to detect Ag<sup>+</sup> with a detection limit of 18 fg mL<sup>-1</sup>.<sup>334</sup> 4-Chloro-1-naphthol was utilized as a substrate, in which the Fe<sub>3</sub>O<sub>4</sub> IONzyme POD enzyme activity was activated in the presence of Ag<sup>+</sup>, which produced the insulating precipitation of benzo-4-chlorohexadienone. The insulating products attenuated the photocurrent signal, reflecting the presence of Ag<sup>+</sup>. Guo *et al.* developed an excellent colorimetric selective method for the detection of Hg<sup>2+</sup> based on the stimulus of the intrinsic oxidase-like catalytic activity of Ag-CoFe<sub>2</sub>O<sub>4</sub>/rGO NPs *via* a one-pot microwave-assisted reaction, which can oxidize 3,3',5,5'-tetramethylbenzidine (TMB) to yield a light-blue product.<sup>335</sup>

Recently, IONzymes have been established as anti-microbial for environmental treatments. IONzymes effectively inactivate viruses (IAVs) *via* envelope lipid peroxidation and destruction of the integrity of neighboring proteins, including hemagglutinin, neuraminidase, and matrix protein. Furthermore, IONzymes possess a broad-spectrum antiviral activity against 12 subtypes of IAVs 244 (H1-H12).<sup>336</sup>

In the treatment of organic pollutants in water, ferromagnetic chitosan IONzymes (MNP@CTS), which have superior catalytic activity and exceptional POD activity, were produced for the degradation of phenol. MNP@CTS removed over 95% of phenol from an aqueous solution within 5 h under the optimum conditions (pH range of 2–10).<sup>337</sup>

Huo *et al.* showed that IONzymes can enhance the performance of plants under unfavorable conditions such as abiotic

stresses. They studied the effect of a 25 ppm IONzyme dose on *Eucalyptus tereticornis* against a high salinity concentration of 300 mM NaCl. The IONzymes showed a separate biochemical change in superoxide dismutase, malondialdehyde concentration, and total soluble sugar and proline content, which are biomarkers that circumvent the stress response and synergistically improve the activity of CAT and POD enzymes.<sup>338</sup>

Recently, Fe<sub>3</sub>O<sub>4</sub>-TiO<sub>2</sub>/reduced graphene oxide (Fe<sub>3</sub>O<sub>4</sub>-TiO<sub>2</sub>/rGO) NPs with hydrogen peroxide activity and photocatalytic efficiency were designed for the colorimetric detection of atrazine pesticides, which can cause long-term negative effects because of their persistence. TMB was used as the substrate compound with a detection limit of 2.98 µg L<sup>-1</sup>.<sup>339</sup> Moreover, the POD-like activity of IONzymes was utilized in water purification in another study.<sup>340–343</sup> This designates the promising application potential of Fe<sub>3</sub>O<sub>4</sub> IONzymes in water treatment and quality analysis.

## 4. Future scope and drawbacks of IONzymes

The future potential as and present limitations of the applications of IONzymes must be considered for their development. IONzymes have enormous potential for use in the environmental and biomedical fields. Employing IONzymes in targeted drug delivery systems and improved diagnostics is one field of research and development that has great potential.<sup>344</sup> Thorek *et al.* suggested that IONzymes may revolutionize magnetic resonance imaging (MRI) by improving the imaging contrast and specificity. However, there are a few issues and disadvantages that need to be resolved. One of the main challenges is still their long-term biocompatibility and toxicity, particularly for *in vivo* applications.<sup>345</sup>

Although iron oxides are considered to be biocompatible in general, Szalay *et al.* proposed that further research is needed to determine their long-term impacts in biological systems.<sup>346</sup> Another serious obstacle is the synthesis of IONzymes on a large scale for industrial use. Researchers emphasized that the shift from laboratory-scale production to large-scale manufacturing frequently leads to instabilities in particle size and enzyme activity, which can hinder their practical implementation.<sup>346</sup>



One more crucial element is the stability of IONzymes in physiological settings. Thus, enhancing their stability through surface modifications, while maintaining their enzymatic activity under various pH and temperature conditions, is crucial for their effective use in biological systems.<sup>38</sup> In addition, achieving high specificity in the catalytic action of IONzymes remains a major research goal. As noted by Zhang and co-workers, tailoring nanozymes to exhibit enzyme-like specificity is a complex but vital aspect for their application in both the medical and environmental fields. Enabling the actual deployment of IONzymes requires addressing these obstacles *via* inventive research and technological developments.<sup>39</sup> To fully utilize the promise of IONzymes in a variety of applications, future research should focus on improving their biocompatibility, scalability, stability, and specificity.<sup>346</sup>

## 5. Conclusion

In conclusion, the study of IONzymes has seen significant advances in recent years. IONzymes can be synthesized using chemical, physical, and biological techniques and offer unique advantages for various applications, including biomedical and environmental purposes. IONzymes have been explored for their enzymatic properties and used in enzyme mimicry, immunoassays, diagnosis, therapy, and biomarker detection. Thus, the versatile nature of IONzymes, combined with their biocompatibility and biodegradability, make them a promising area for continued research and development.

## Author contributions

Ghazzy A, conceptualization, writing – original draft, writing, review & editing, supervision; Nsairat H, writing – original draft; Said R, writing – original draft, writing, review & editing; Sibai O, writing – original draft, resources; AbuRuman A, writing – original draft; Shraim A, visualization & editing; Al hunaiti A, conceptualization.

## Conflicts of interest

There are no conflicts to declare.

## Acknowledgements

A. G. would like to acknowledge support by Deanship of Scientific Research at Al-Ahliyya Amman University. A. A.-H. Acknowledges support by the Deanship of Scientific Research at the University of Jordan.

## References

- G. A. Silva, Introduction to nanotechnology and its applications to medicine, *Surg. Neurol.*, 2004, **61**, 216–220.
- V. Amendola and M. Meneghetti, What controls the composition and the structure of nanomaterials generated by laser ablation in liquid solution?, *Phys. Chem. Chem. Phys.*, 2013, **15**, 3027–3046.
- B. T. Sone, A. Diallo, X. G. Fuku, A. Gurib-Fakim and M. Maaza, Biosynthesized CuO nano-platelets: Physical properties & enhanced thermal conductivity nanofluidics, *Arabian J. Chem.*, 2020, **13**, 160–170.
- A. U. Khan, M. Khan, N. Malik, M. H. Cho and M. M. Khan, Recent progress of algae and blue-green algae-assisted synthesis of gold nanoparticles for various applications, *Bioprocess Biosyst. Eng.*, 2019, **42**, 1–15.
- A. Ash, K. Revati and B. D. Pandey, Microbial synthesis of iron-based nanomaterials – A review, *Bull. Mater. Sci.*, 2011, **34**, 191–198.
- H. Geng, Y. Peng, L. Qu, H. Zhang and M. Wu, Structure Design and Composition Engineering of Carbon-Based Nanomaterials for Lithium Energy Storage, *Adv. Energy Mater.*, 2020, **10**, 1–34.
- X. Zhang, W. Li, H. Kou, J. Shao, Y. Deng, X. Zhang, J. Ma, Y. Li and X. Zhang, Temperature and size dependent surface energy of metallic nano-materials, *J. Appl. Phys.*, 2019, **125**, 185105.
- S. Dang, Q. L. Zhu and Q. Xu, Nanomaterials derived from metal-organic frameworks, *Nat. Rev. Mater.*, 2017, **3**, 1–14.
- J. T. Lue, A review of characterization and physical property studies of metallic nanoparticles, *J. Phys. Chem. Solids*, 2001, **62**, 1599–1612.
- V. V. Mody, R. Siwale, A. Singh and H. R. Mody, Introduction to metallic nanoparticles, *J. Pharm. BioAllied Sci.*, 2010, **2**, 282–289.
- K. I. Bogutskaya, Y. P. Sklyarov and Y. I. Prylutskyy, Zinc and zinc nanoparticles : biological role and application in biomedicine, *Ukrainica Bioorganica Acta*, 2013, **1**, 9–16.
- S. G. Kim, Y. Terashi, A. Purwanto and K. Okuyama, Synthesis and film deposition of Ni nanoparticles for base metal electrode applications, *Colloids Surf.*, 2009, **337**, 96–101.
- M. Parashar, V. K. Shukla and R. Singh, Metal oxides nanoparticles *via* sol-gel method: a review on synthesis, characterization and applications, *J. Mater.*, 2020, **31**, 3729–3749.
- S. U. Son, I. K. Park, P. Jongnam and T. Hyeon, Synthesis of Cu<sub>2</sub>O coated Cu nanoparticles and their successful applications to Ullmann-type amination coupling reactions of aryl chlorides, *Chem. Commun.*, 2004, **4**, 778–779.
- A. Rita, A. Sivakumar, S. S. J. Dhas and S. A. M. B. Dhas, Structural, optical and magnetic properties of silver oxide (AgO) nanoparticles at shocked conditions, *J. Nanostruct. Chem.*, 2020, **10**, 309–316.
- B. P. Vinayan and S. Ramaprabhu, Facile synthesis of SnO<sub>2</sub> nanoparticles dispersed nitrogen doped graphene anode material for ultrahigh capacity lithium ion battery applications, *J. Mater. Chem. A*, 2013, **1**, 3865–3871.
- B. Mughal, S. Z. J. Zaidi, X. Zhang and S. U. Hassan, Biogenic nanoparticles: Synthesis, characterisation and applications, *Appl. Sci.*, 2021, **11**, 2598.
- M. Mahdavi, M. B. Ahmad, M. J. Haron, F. Namvar, B. Nadi, M. Z. Ab Rahman and J. Amin, Synthesis, surface modification and characterisation of biocompatible



- magnetic iron oxide nanoparticles for biomedical applications, *Molecules*, 2013, **18**, 7533–7548.
- 19 D. Ling and T. Hyeon, Iron Oxide Nanoparticles Chemical Design of Biocompatible Iron Oxide Nanoparticles for Medical Applications, *Small*, 2013, **9**, 1449.
  - 20 M. A. Wahab, S. M. A. Hossain, M. K. Masud, H. Park, A. Ashok, M. Mustapić, M. Kim, D. Patel, M. Shahbazi and M. S. A. Hossain, Nanoarchitected superparamagnetic iron oxide-doped mesoporous carbon nanozymes for glucose sensing, *Sens. Actuators, B*, 2022, **366**, 131980.
  - 21 Q. Chen, X. Zhang, S. Li, J. Tan, C. Xu and Y. Huang, MOF-derived  $\text{Co}_3\text{O}_4$ @Co-Fe oxide double-shelled nanocages as multi-functional specific peroxidase-like nanozyme catalysts for chemo/biosensing and dye degradation, *Chem. Eng. J.*, 2020, **395**, 125130.
  - 22 Y. Wang, W. Wang, Z. Gu, X. Miao, Q. Huang and B. Chang, Temperature-responsive iron nanozymes based on poly(N-vinylcaprolactam) with multi-enzyme activity, *RSC Adv.*, 2020, **10**, 39954–39966.
  - 23 Y. Lin, J. Ren and X. Qu, Catalytically active nanomaterials: A promising candidate for artificial enzymes, *Acc. Chem. Res.*, 2014, **47**, 1097–1105.
  - 24 T. Kang, Y. G. Kim, D. Kim and T. Hyeon, Inorganic nanoparticles with enzyme-mimetic activities for biomedical applications, *Coord. Chem. Rev.*, 2020, **403**, 213092.
  - 25 K. Boriachek, M. K. Masud, C. Palma, H. P. Phan, Y. Yamauchi, M. S. A. Hossain, N. T. Nguyen, C. Salomon and M. J. A. Shiddiky, Avoiding pre-isolation step in exosome analysis: Direct isolation and sensitive detection of exosomes using gold-loaded nanoporous ferric oxide nanozymes, *Anal. Chem.*, 2019, **91**, 3827–3834.
  - 26 P. Wang, T. Wang, J. Hong, X. Yan and M. Liang, Nanozymes: A New Disease Imaging Strategy, *Front. Bioeng. Biotechnol.*, 2020, **8**, 1–10.
  - 27 B. Wang, A. Moyano, J. M. Duque, L. Sánchez, G. García-Santos, L. J. G. Flórez, E. Serrano-Pertierra and M. D. C. Blanco-López, Nanozyme-Based Lateral Flow Immunoassay (LFIA) for Extracellular Vesicle Detection, *Biosensors*, 2022, **12**, 1–13.
  - 28 Z. Nie, Y. Vahdani, W. C. Cho, S. H. Bloukh, Z. Edis, S. Haghighat, M. Falahati, R. Kheradmandi, L. A. Jaragh-Alhadad and M. Sharifi, 5-Fluorouracil-containing inorganic iron oxide/platinum nanozymes with dual drug delivery and enzyme-like activity for the treatment of breast cancer, *Arabian J. Chem.*, 2022, **15**, 103966.
  - 29 Y. He, X. Chen, Y. Zhang, Y. Wang, M. Cui, G. Li, X. Liu and H. Fan, Magneto-responsive nanozyme: magnetic stimulation on the nanozyme activity of iron oxide nanoparticles, *Sci. China Life Sci.*, 2021, **65**, 184–192.
  - 30 G. Tang, J. He, J. Liu, X. Yan, K. Fan and C. Xiyun Yan, Nanozyme for tumor therapy: Surface modification matters, *Exploration*, 2021, **1**, 75–89.
  - 31 K. Fan, H. Wang, J. Xi, Q. Liu, X. Meng, D. Duan, L. Gao and X. Yan, Optimization of  $\text{Fe}_3\text{O}_4$  nanozyme activity via single amino acid modification mimicking an enzyme active site, *Chem. Commun.*, 2016, **53**(2), 424–427.
  - 32 R. Zhang, H. Zhao, and K. Fan, in *Nanozymes: Design, Synthesis, and Applications*, ed. X. Wang, American Chemical Society, Washington, DC, first edition, 2022, ch. 1, pp. 1–35.
  - 33 Y. Chen, J. Zhang, Z. Wang and Z. Zhou, Solvothermal Synthesis of Size-Controlled Monodispersed Superparamagnetic Iron Oxide Nanoparticles, *Appl. Sci.*, 2019, **9**, 5157.
  - 34 H. Zou, J. Zhao, F. He, Z. Zhong, J. Huang, Y. Zheng, Y. Zhang, Y. Yang, F. Yu, M. A. Bashir and B. Gao, Ball milling biochar iron oxide composites for the removal of chromium (Cr(VI)) from water: Performance and mechanisms, *J. Hazard. Mater.*, 2021, **413**, 125252.
  - 35 L. Gao, J. Zhuang, L. Nie, J. Zhang, Y. Zhang, N. Gu, T. Wang, J. Feng, D. Yang, S. Perrett and X. Yan, Intrinsic peroxidase-like activity of ferromagnetic nanoparticles, *Nat. Nanotechnol.*, 2007, **2**, 577–583.
  - 36 M. Wu, H. Guo, L. Liu, Y. Liu and L. Xie, Size-dependent cellular uptake and localization profiles of silver nanoparticles, *Int. J. Nanomed.*, 2019, **14**, 4247–4259.
  - 37 H. Wei and E. Wang,  $\text{Fe}_3\text{O}_4$  magnetic nanoparticles as peroxidase mimetics and their applications in  $\text{H}_2\text{O}_2$  and glucose detection, *Anal. Chem.*, 2008, **80**, 2250–2254.
  - 38 S. Laurent, D. Forge, M. Port, A. Roch, C. Robic, L. Vander Elst and R. N. Muller, Magnetic iron oxide nanoparticles: synthesis, stabilization, vectorization, physicochemical characterizations, and biological applications, *Chem. Rev.*, 2008, **108**, 2064–2110.
  - 39 S. Zhang, X. Zhang, G. Jiang, H. Zhu, S. Guo, D. Su, G. Lu and S. Sun, Tuning nanoparticle structure and surface strain for catalysis optimization, *J. Am. Chem. Soc.*, 2014, **136**, 7734–7739.
  - 40 T. Athar, in *Emerging Nanotechnologies for Manufacturing*, ed. W. Ahmed and M. J. Jackson, William Andrew Publishing, Elsevier Inc, second edition, 2015, ch. 17, pp. 444–538.
  - 41 N. S. Satpute and S. J. Dhoble, in *Energy Materials: Fundamentals to Applications*, ed. S. J. Dhoble, N. T. Kalyani, B. Vengadaesvaran and A. K. Arof, Elsevier, first edition, 2021, ch. 14, pp. 407–444.
  - 42 J. Chang, Y. L. Zhou and Y. Zhou, in *Bioactive Glasses: Materials, Properties and Applications*, ed. H. O. Ylänen, Woodhead Publishing, first edition, 2011, ch. 2, pp. 29–52.
  - 43 A. Sarkar, N. Saha and G. Majumdar, in *Encyclopedia of Materials: Plastics and Polymers*, ed. M. S. J. Hashmi, Elsevier Inc, first edition, 2022, vol. 2, pp. 646–655.
  - 44 R. Massart, Preparation of Aqueous Magnetic Liquids in Alkaline and Acidic Media, *IEEE Trans. Magn.*, 1981, **17**, 1247–1248.
  - 45 J. C. Apesteguy, G. V. Kurlyandskaya, J. P. De Celis, A. P. Safronov and N. N. Schegoleva, Magnetite nanoparticles prepared by co-precipitation method in different conditions, *Mater. Chem. Phys.*, 2015, **161**, 243–249.



- 46 S. Laurent, D. Forge, M. Port, A. Roch, C. Robic, L. Vander Elst and R. N. Muller, Magnetic iron oxide nanoparticles: synthesis, stabilization, vectorization, physicochemical characterizations, and biological applications, *Chem. Rev.*, 2008, **108**, 2064–2110.
- 47 A. M. Mazrouaa, M. G. Mohamed and M. Fekry, Physical and magnetic properties of iron oxide nanoparticles with a different molar ratio of ferrous and ferric, *Egypt. J. Pet.*, 2019, **28**, 165–171.
- 48 S. P. Schwaminger, C. Syhr and S. Berensmeier, Controlled Synthesis of Magnetic Iron Oxide Nanoparticles: Magnetite or Maghemite?, *Crystals*, 2020, **10**, 214.
- 49 A. V. Samrot, C. S. Sahithya, A. J. Selvarani, S. K. Purayil and P. Ponnaiah, A review on synthesis, characterization and potential biological applications of superparamagnetic iron oxide nanoparticles, *Curr. Res. Green Sustainable Chem.*, 2021, **4**, 100042.
- 50 M. O. Besenhard, A. P. LaGrow, A. Hodzic, M. Kriechbaum, L. Panariello, G. Bais, K. Loizou, S. Damilos, M. M. Cruz, N. T. K. Thanh and A. Gavriilidis, Co-precipitation synthesis of stable iron oxide nanoparticles with NaOH: New insights and continuous production *via* flow chemistry, *Chem. Eng. J.*, 2020, **399**, 125740.
- 51 A. P. Lagrow, M. O. Besenhard, A. Hodzic, A. Sergides, L. K. Bogart, A. Gavriilidis and N. T. K. Thanh, Unravelling the growth mechanism of the co-precipitation of iron oxide nanoparticles with the aid of synchrotron X-Ray diffraction in solution, *Nanoscale*, 2019, **11**, 6620–6628.
- 52 B. Chen, J. Sun, F. Fan, X. Zhang, Z. Qin, P. Wang, Y. Li, X. Zhang, F. Liu, Y. Liu, M. Ji and N. Gu, Ferumoxytol of ultrahigh magnetization produced by hydrocooling and magnetically internal heating co-precipitation, *Nanoscale*, 2018, **10**, 7369–7376.
- 53 I. Nkurikiyimfura, Y. Wang, B. Safari and E. Nshingabigwi, Temperature-dependent magnetic properties of magnetite nanoparticles synthesized *via* coprecipitation method, *J. Alloys Compd.*, 2020, **846**, 156344.
- 54 L. B. de Mello, L. C. Varanda, F. A. Sigoli and I. O. Mazali, Co-precipitation synthesis of (Zn-Mn)-co-doped magnetite nanoparticles and their application in magnetic hyperthermia, *J. Alloys Compd.*, 2019, **779**, 698–705.
- 55 M. Aliofkhaezrai, *Handbook of Nanoparticles*, Springer Cham, Switzerland, 2015.
- 56 H. Hayashi and Y. Hakuta, Hydrothermal Synthesis of Metal Oxide Nanoparticles in Supercritical Water, *Materials*, 2010, **3**, 3794–3817.
- 57 S. Takami, T. Sato, T. Mousavand, S. Ohara, M. Umetsu and T. Adschiri, Hydrothermal synthesis of surface-modified iron oxide nanoparticles, *Mater. Lett.*, 2007, **61**, 4769–4772.
- 58 M. O'Donoghue, *A Guide to Man-Made Gemstones*, Van Nostrand Reinhold, New York, 1983.
- 59 D. A. Brewster, D. J. Sarappa and K. E. Knowles, Role of aliphatic ligands and solvent composition in the solvothermal synthesis of iron oxide nanocrystals, *Polyhedron*, 2019, **157**, 54–62.
- 60 O. S. Hammond, R. S. Atri, D. T. Bowron, L. De Campo, S. Diaz-Moreno, L. L. Keenan, J. Douth, S. Eslava and K. J. Edler, Structural evolution of iron forming iron oxide in a deep eutectic-solvothermal reaction, *Nanoscale*, 2021, **13**, 1723.
- 61 J. González-Rivera, A. Spepi, C. Ferrari, J. Tovar-Rodríguez, E. Fantechi, F. Pineider, M. A. Vera-Ramírez, M. R. Tiné and C. Duce, Magnetothermally-responsive nanocarriers using confined phosphorylated halloysite nanoreactor for *in situ* iron oxide nanoparticle synthesis: A MW-assisted solvothermal approach, *Colloids Surf., A*, 2022, **635**, 128116.
- 62 Y.-Y. Zheng, Q. Sun, Y.-H. Duan, J. Zhai, L.-L. Zhang and J.-X. Wang, Controllable synthesis of monodispersed iron oxide nanoparticles by an oxidation-precipitation combined with solvothermal process, *Mater. Chem. Phys.*, 2020, **252**, 123431.
- 63 D. Gusain, O. O. Awolusi and F. Bux, Synthesis and characterization of iron oxide/MIL-101 composite *via* microwave solvothermal treatment, *Surf. Sci.*, 2022, **716**, 121952.
- 64 L. Besra and M. Liu, A review on fundamentals and applications of electrophoretic deposition (EPD), *Prog. Mater. Sci.*, 2007, **52**, 1–6.
- 65 H. Kang, Y. Park, Y. K. Hong, S. Yoon, M. H. Lee and D. H. Ha, Solvent-induced charge formation and electrophoretic deposition of colloidal iron oxide nanoparticles, *Surf. Interfaces*, 2021, **22**, 100815.
- 66 S. C. Mills, C. S. Smith, D. P. Arnold and J. S. Andrew, Electrophoretic deposition of iron oxide nanoparticles to achieve thick nickel/iron oxide magnetic nanocomposite films, *AIP Adv.*, 2020, **10**, 15308.
- 67 S. Singh, G. Singh and N. Bala, Characterization, electrochemical behavior and *in vitro* hemocompatibility of hydroxyapatite-bioglass-iron oxide-chitosan composite coating by electrophoretic deposition, *Surf. Coat. Technol.*, 2021, **405**, 126564.
- 68 N. Ugemuge, Y. R. Parauha and S. J. Dhoble, in *Energy Materials: Fundamentals to Applications*, ed. S. J. Dhoble, N. T. Kalyani, B. Vengadaesvaran and A. K. Arof, Elsevier, first edition, 2021, ch. 15, pp. 445–480.
- 69 Q. Wu, L. He, Z. W. Jiang, Y. Li, Z. M. Cao, C. Z. Huang and Y. F. Li, CuO nanoparticles derived from metal-organic gel with excellent electrocatalytic and peroxidase-mimicking activities for glucose and cholesterol detection, *Biosens. Bioelectron.*, 2019, **145**, 111704.
- 70 R. Rasheed, H. Kareem and H. Mansoor, Preparation and Characterization of Hematite Iron Oxide ( $\alpha$ -Fe<sub>2</sub>O<sub>3</sub>) by Sol-Gel Method, *Chem. Sci. J.*, 2018, **9**, 1000197.
- 71 S. Yasnur, P. Maji, A. Ray, H. Mullick and S. Das, Effect of annealing temperature on dielectric properties of iron oxide prepared by sol-gel auto combustion method, *Ferroelectrics*, 2021, **577**, 38–51.
- 72 D. Bokov, A. T. Jalil, S. Chupradit, W. Suksatan, M. J. Ansari, I. H. Shewael, G. H. Valiev and E. Kianfar, Nanomaterial by Sol-Gel Method: Synthesis and Application, *Adv. Mater. Sci. Eng.*, 2021, **2021**, 1–21.
- 73 A. Akbar, H. Yousaf, S. Riaz and S. Naseem, Role of precursor to solvent ratio in tuning the magnetization of



- iron oxide thin films – A sol-gel approach, *J. Magn. Magn. Mater.*, 2019, **471**, 14–24.
- 74 S. Khalid, S. Riaz, S. Naeem, A. Akbar, S. S. Hussain, Y. B. Xu and S. Naseem, Spin polarization and magneto-dielectric coupling in Al-modified thin iron oxide films-microwave mediated sol-gel approach, *J. Ind. Eng. Chem.*, 2021, **103**, 49–66.
- 75 J. López-Sánchez, A. Serrano, A. Del Campo, M. Abuín, E. Salas-Colera, A. Muñoz-Noval, G. R. Castro, J. De La Figuera, J. F. Marco, P. Marín, N. Carmona and O. Rodríguez de la Fuente, Self-assembly of iron oxide precursor micelles driven by magnetic stirring time in sol-gel coatings, *RSC Adv.*, 2019, **9**, 17571–17580.
- 76 Y. L. Liu, Y. T. Li, J. F. Huang, Y. L. Zhang, Z. H. Ruan, T. Hu, J. J. Wang, W. Y. Li, H. J. Hu and G. B. Jiang, An advanced sol-gel strategy for enhancing interfacial reactivity of iron oxide nanoparticles on rosin biochar substrate to remove Cr(VI), *Sci. Total Environ.*, 2019, **690**, 438–446.
- 77 G. P. Ricci, L. O. Garcia, E. J. Nassar, S. Nakagaki, J. F. Stival, Z. Novaes da Rocha, M. A. Vicente, R. Trujillano, A. Jiménez, V. Rives, L. Marçal, E. Henrique de Faria and K. J. Ciuffi, Non-hydrolytic sol-gel synthesis of mesoporous iron-aluminum oxide and their properties in the oxidation of hydrocarbons by hydrogen peroxide, *Microporous Mesoporous Mater.*, 2021, **325**, 111317.
- 78 G. A. Marcelo, C. Lodeiro, J. L. Capelo, J. Lorenzo and E. Oliveira, Magnetic, fluorescent and hybrid nanoparticles: From synthesis to application in biosystems, *Mater. Sci. Eng., C*, 2020, **106**, 110104.
- 79 A. Erwin, S. Salomo, P. Adhy, N. Utari, W. Ayu, Y. Wita and S. Nani, Magnetic iron oxide particles (Fe<sub>3</sub>O<sub>4</sub>) fabricated by ball milling for improving the environmental quality, *IOP Conf. Ser.: Mater. Sci. Eng.*, 2020, **845**, 012051.
- 80 H. S. Woon, L. S. Ewe, K. P. Lim and I. Ismail, Synthesis and Characterization of Iron Oxide Waste-Derived Red Colour Pigment via Cryo-Milling Process, *Asian J. Appl. Sci.*, 2020, **1**, 22–28.
- 81 A. Younes, N. Dilmi and A. Bouamer, Effect of zinc oxide and alumina nanoparticles on Structural, magnetic and mechanical properties of the iron matrix synthesized by mechanical milling and thermal spraying, *Mater. Today: Proc.*, 2021, **42**, 2990–2995.
- 82 S. Liu, B. Yu, S. Wang, Y. Shen and H. Cong, Preparation, surface functionalization and application of Fe<sub>3</sub>O<sub>4</sub> magnetic nanoparticles, *Adv. Colloid Interface Sci.*, 2020, **281**, 102165.
- 83 P. G. Jamkhande, N. W. Ghule, A. H. Bamer and M. G. Kalaskar, Metal nanoparticles synthesis: An overview on methods of preparation, advantages and disadvantages, and applications, *J. Drug Delivery Sci. Technol.*, 2019, **53**, 101174.
- 84 X. Fu, J. Cai, X. Zhang, W.-D. Li, H. Ge and Y. Hu, Top-down fabrication of shape-controlled, monodisperse nanoparticles for biomedical applications, *Adv. Drug Delivery Rev.*, 2018, **132**, 169–187.
- 85 T. Cele, in *Engineered Nanomaterials-Health and Safety*, ed. S. M. Avramescu, K. Akhtar, I. Fierascu, S. B. Khan, F. Ali and A. M. Asiri, IntechOpen, London, 2020, ch. 2, pp. 15–28.
- 86 V. Amendola, P. Riello and M. Meneghetti, Magnetic Nanoparticles of Iron Carbide, Iron Oxide, Iron@Iron Oxide, and Metal Iron Synthesized by Laser Ablation in Organic Solvents, *J. Phys. Chem. C*, 2011, **115**, 5140–5146.
- 87 X. Luo, A. H. M. Al-Antaki, T. M. D. Alharbi, W. D. Hutchison, Y.-C. Zou, J. Zou, A. Sheehan, W. Zhang and C. L. Raston, Laser-Ablated Vortex Fluidic-Mediated Synthesis of Superparamagnetic Magnetite Nanoparticles in Water Under Flow, *ACS Omega*, 2018, **3**, 11172–11178.
- 88 M. James, R. A. Revia, Z. Stephen and M. Zhang, Microfluidic Synthesis of Iron Oxide Nanoparticles, *Nanomaterials*, 2020, **10**, 2113.
- 89 R. Chandra, A. K. Chawla and P. Ayyub, Optical and structural properties of sputter-deposited nanocrystalline Cu<sub>2</sub>O films: effect of sputtering gas, *J. Nanosci. Nanotechnol.*, 2006, **6**, 1119–1123.
- 90 Q. Chen, H. Wang, S. Perero, Q. Wang, Q. Chen and Q. Structural, optical and magnetic properties of Fe<sub>3</sub>O<sub>4</sub> sputtered TeO<sub>2</sub>-PbO-B<sub>2</sub>O<sub>3</sub> and PbO-Bi<sub>2</sub>O<sub>3</sub>-B<sub>2</sub>O<sub>3</sub> glasses for sensing applications, *J. Non-Cryst. Solids*, 2015, **408**, 43–50.
- 91 P. Nie, G. Xu, J. Jiang, H. Dou, Y. Wu, Y. Zhang, J.-F. Wang, M. Shi, R. Fu and X. Zhang, Aerosol-Spray Pyrolysis toward Preparation of Nanostructured Materials for Batteries and Supercapacitors, *Small Methods*, 2018, **2**, 1700272.
- 92 A.-G. Niculescu, C. Chircov and A. M. Grumezescu, Magnetite nanoparticles: Synthesis methods – A comparative review, *Methods*, 2022, **199**, 16–27.
- 93 T. V. Gavrilović, D. J. Jovanović and M. D. Dramićanin, in *Nanomaterials for Green Energy: A Volume of Micro and Nano Technologies*, ed. B. A. Bhanvase, V. B. Pawade, S. J. Dhoble, S. H. Sonawane and M. Ashokkumar, Elsevier, 2018, ch. 2, pp. 55–81.
- 94 L. T. Govindaraman, A. Arjunan, A. Baroutaji, J. Robinson, M. Ramadan and A. G. Olabi, Nanomaterials Theory and Applications, *Encyclopedia of Smart Materials*, 2022, vol. 3, pp. 302–314.
- 95 S. K. Das, S. Chakraborty, S. Naskar and R. Rajabalaya, in *Bionanocomposites in Tissue Engineering and Regenerative Medicine: A Volume in Woodhead Publishing Series in Biomaterials*, ed. S. Ahmed and Annu, Woodhead Publishing, 2021, ch. 3, pp. 17–43.
- 96 Z. Ferdous, M. S. Ullah and S. Hussain, Temperature and Substrate Effects on the Structural, Morphological, and Optical Properties of Iron Oxide Thin Films Prepared by Spray Pyrolysis Technique, *Dhaka Univ. J. Sci.*, 2020, **68**, 79–85.
- 97 A. S. Hassanien and A. A. Akl, Optical characteristics of iron oxide thin films prepared by spray pyrolysis technique at different substrate temperatures, *Appl. Phys. A*, 2018, **124**, 752.
- 98 R. Tischendorf, M. Simmler, C. Weinberger, M. Bieber, M. Reddemann, F. Fröde, J. Lindner, H. Pitsch, R. Kneer, M. Tiemann, H. Nirschl and H.-J. Schmid, Examination of



- the evolution of iron oxide nanoparticles in flame spray pyrolysis by tailored *in situ* particle sampling techniques, *J. Aerosol Sci.*, 2021, **154**, 105722.
- 99 J. Zheng, K. Liu, W. Cai, L. Qiao, Y. Ying, W. Li, J. Yu, M. Lin and S. Che, Effect of chloride ion on crystalline phase transition of iron oxide produced by ultrasonic spray pyrolysis, *Adv. Powder Technol.*, 2018, **29**, 1953–1959.
- 100 A. T. Hassan and E. S. Hassan, Effect of Thickness on Crystal Structure and Dispersion Parameters of Haematite Iron Oxide by Spray Pyrolysis Technique, *Acta Phys. Pol., A*, 2021, **140**, 295–298.
- 101 J. Xie, Y. Guo, S. Lou, Z. Wei, P. Hao, F. Lei and B. Tang, A molten-salt protected pyrolysis approach for fabricating a ternary nickel-cobalt-iron oxide nanomesh catalyst with promoted oxygen-evolving performance, *Chem. Commun.*, 2020, **56**, 4579–4582.
- 102 M. F. B. Stodt, C. Liu, S. Li, L. Mädler, U. Fritsching and J. Kiefer, Phase-selective laser-induced breakdown spectroscopy in flame spray pyrolysis for iron oxide nanoparticle synthesis, *Proc. Combust. Inst.*, 2021, **38**, 1711–1718.
- 103 N. Priya, K. Kaur and A. K. Sidhu, Green Synthesis: An Eco-friendly Route for the Synthesis of Iron Oxide Nanoparticles, *Frontal Nanotechnol.*, 2021, **3**, 655062.
- 104 S. Perveen, R. Nadeem, S. Rehman, N. Afzal, S. Anjum, S. Noreen, R. Saeed, M. Amami, M. S. H. Al-Mijalli and M. Iqbal, Green synthesis of iron (Fe) nanoparticles using *Plumeria obtusa* extract as a reducing and stabilizing agent: Antimicrobial, antioxidant and biocompatibility studies, *Arabian J. Chem.*, 2022, **15**, 103764.
- 105 N. A. Zakariya, S. Majeed and W. H. W. Jusof, Investigation of antioxidant and antibacterial activity of iron oxide nanoparticles (IONPS) synthesized from the aqueous extract of *Penicillium* spp, *Sens. Int.*, 2022, **3**, 100164.
- 106 M. S. Samuel, S. Datta, N. Chandrasekar, R. Balaji, E. Selvarajan and S. Vuppala, Biogenic Synthesis of Iron Oxide Nanoparticles Using *Enterococcus faecalis*: Adsorption of Hexavalent Chromium from Aqueous Solution and *In Vitro* Cytotoxicity Analysis, *Nanomaterials*, 2021, **11**, 3290.
- 107 S. M. Shalaby, F. F. Madkour, H. Y. El-Kassas, A. A. Mohamed and A. M. Elgarahy, Green synthesis of recyclable iron oxide nanoparticles using *Spirulina platensis* microalgae for adsorptive removal of cationic and anionic dyes, *Environ. Sci. Pollut. Res.*, 2021, **28**, 65549–65572.
- 108 M. Noruzi, Biosynthesis of gold nanoparticles using plant extracts, *Bioprocess Biosyst. Eng.*, 2015, **38**, 1–14.
- 109 A. K. Mittal, Y. Chisti and U. C. Banerjee, Synthesis of metallic nanoparticles using plant extracts, *Biotechnol. Adv.*, 2013, **31**, 346–356.
- 110 S. Roy and T. K. Das, Plant Mediated Green Synthesis of Silver Nanoparticles-A Review, *Int. J. Plant Biol.*, 2015, **3**, 1044–1055.
- 111 H. Agarwal, S. V. Kumar and S. Rajeshkumar, A review on green synthesis of zinc oxide nanoparticles-An eco-friendly approach, *Resour.-Effic. Technol.*, 2017, **3**, 406–413.
- 112 A. U. Mirza, A. Kareem, S. A. A. Nami, M. S. Khan, S. Rehman, S. A. Bhat, A. Mohammad and N. Nishat, Biogenic synthesis of iron oxide nanoparticles using *Aegle marmelos* and *Prunus persica* phyto species: Characterization, antibacterial and antioxidant activity, *J. Photochem. Photobiol. B, Biol.*, 2018, **185**, 262–274.
- 113 M. Nadeem, D. Tungmunnithum, C. Hano, B. H. Abbasi, S. S. Hashmi, W. Ahmad and A. Zahir, The current trends in the green syntheses of titanium oxide nanoparticles and their applications, *Green Chem. Lett. Rev.*, 2018, **11**, 492–502.
- 114 S. Vasantharaj, S. Sathiyavimal, P. Senthilkumar, F. LewisOscar and A. Pugazhendhi, Biosynthesis of iron oxide nanoparticles using leaf extract of *Ruellia tuberosa*: Antimicrobial properties and their applications in photocatalytic degradation, *J. Photochem. Photobiol. B, Biol.*, 2019, **192**, 74–82.
- 115 P. Mondal, A. Anweshan and M. K. Purkait, Green synthesis and environmental application of iron-based nanomaterials and nanocomposite: A review, *Chemosphere*, 2020, **259**, 127509.
- 116 K. Kaur and A. K. Sidhu, Green synthesis: An eco-friendly route for the synthesis of iron oxide nanoparticles, *Frontal Nanotechnol.*, 2021, **3**, 655062.
- 117 S. A. Razack, A. Suresh, S. Sriram, G. Ramakrishnan, S. Sadanandham, M. Veerasamy, R. B. Nagalamadaka and R. Sahadevan, Green synthesis of iron oxide nanoparticles using *Hibiscus rosa-sinensis* for fortifying wheat biscuits, *SN Appl. Sci.*, 2020, **2**, 898.
- 118 M. S. H. Bhuiyan, M. Y. Miah, S. C. Paul, T. D. Aka, O. Saha, M. M. Rahaman, M. J. I. Sharif, O. Habiba and M. Ashaduzzaman, Green synthesis of iron oxide nanoparticle using *Carica papaya* leaf extract: application for photocatalytic degradation of remazol yellow RR dye and antibacterial activity, *Heliyon*, 2020, **6**, e04603.
- 119 N. Madubuonu, S. O. Aisida, I. Ahmad, S. Botha, T.-K. Zhao, M. Maaza and F. I. Ezema, Bio-inspired iron oxide nanoparticles using *Psidium guajava* aqueous extract for antibacterial activity, *Appl. Phys. A*, 2020, **126**, 1–8.
- 120 R. Hooda and M. Sharma, Green synthesis, characterization and antibacterial activity of iron oxide nanoparticles, *Plant Arch.*, 2020, **20**, 1196–1200.
- 121 A. S. Y. Ting and J. E. Chin, Biogenic Synthesis of Iron Nanoparticles from Apple Peel Extracts for Decolorization of Malachite Green Dye, *Water, Air, Soil Pollut.*, 2020, **231**, 278.
- 122 B. Kumar, K. Smita, S. Galeas, V. Sharma, V. H. Guerrero, A. Debut and L. Cumbal, Characterization and application of biosynthesized iron oxide nanoparticles using *Citrus paradisi* peel: A sustainable approach, *Inorg. Chem. Commun.*, 2020, **119**, 108116.
- 123 M. A. Asghar, E. Zahir, M. A. Asghar, J. Iqbal and A. A. Rehman, Facile, one-pot biosynthesis and characterization of iron, copper and silver nanoparticles using *Syzygium cumini* leaf extract: as an effective antimicrobial and aflatoxin B1 adsorption agents, *PLoS One*, 2020, **15**, e0234964.



- 124 Z. Izadiyan, K. Shameli, M. Miyake, H. Hara, S. E. B. Mohamad, K. Kalantari, S. H. M. Taib and E. Rasouli, Cytotoxicity assay of plant-mediated synthesized iron oxide nanoparticles using Juglans regia green husk extract, *Arabian J. Chem.*, 2020, **13**, 2011–2023.
- 125 K. Rong, J. Wang, Z. Zhang and J. Zhang, Green synthesis of iron nanoparticles using Korla fragrant pear peel extracts for the removal of aqueous Cr(VI), *Ecol. Eng.*, 2020, **149**, 105793.
- 126 D. Patiño-Ruiz, L. Sánchez-Botero, L. Tejeda-Benitez, J. Hinestroza and A. Herrera, Green synthesis of iron oxide nanoparticles using Cymbopogon citratus extract and sodium carbonate salt: Nanotoxicological considerations for potential environmental applications, *Environ. Nanotechnol., Monit. Manage.*, 2020, **14**, 100377.
- 127 M. Jamzad and M. Kamari Bidkorpheh, Green synthesis of iron oxide nanoparticles by the aqueous extract of Laurus nobilis L. leaves and evaluation of the antimicrobial activity, *J. Nanostructure Chem.*, 2020, **10**, 193–201.
- 128 H. E. A. Mohamed, S. Afridi, A. T. Khalil, M. Ali, T. Zohra, M. Salman, A. Ikram, Z. K. Shinwari and M. Maaza, Bio-redox potential of Hyphaene thebaica in bio-fabrication of ultrafine maghemite phase iron oxide nanoparticles (Fe<sub>2</sub>O<sub>3</sub> NPs) for therapeutic applications, *Mater. Sci. Eng., C*, 2020, **112**, 110890.
- 129 D. Bharathi, S. Preethi, K. Abarna, M. Nithyasri, P. Kishore and K. Deepika, Bio-inspired synthesis of flower shaped iron oxide nanoparticles (FeONPs) using phytochemicals of Solanum lycopersicum leaf extract for biomedical applications, *Biocatal. Agric. Biotechnol.*, 2020, **27**, 101698.
- 130 C. Noorjahan, Photosynthesis, Characterization and Antimicrobial Activity of Iron Oxide Nanoparticle using Henna (Lawsonia Inermis), *Int. J. Eng. Sci.*, 2020, **7**, 38–45.
- 131 N. K. Abbas and A. A. Al-Attraqchi, Antimicrobial Activities of Green Biosynthesized Iron Oxide Nanoparticles Using F. Carica Fruit Extract, *Indian J. Forensic Med. Toxicol.*, 2020, **14**, 2181–2187.
- 132 B. A. Abbasi, J. Iqbal, S. A. Zahra, A. Shahbaz, S. Kanwal, A. Rabbani and T. Mahmood, Bioinspired synthesis and activity characterization of iron oxide nanoparticles made using Rhamnus Triquetra leaf extract, *Mater. Res. Express*, 2020, **6**, 1250e1257.
- 133 M. A. Abid, D. A. Kadhim and W. J. Aziz, Iron oxide nanoparticle synthesis using trigonella and tomato extracts and their antibacterial activity, *Mater. Technol.*, 2022, **37**, 547–554.
- 134 W. Aziz, M. Abid, D. Kadhim and M. Mejbil, Synthesis of iron oxide (β-Fe<sub>2</sub>O<sub>3</sub>) nanoparticles from Iraqi grapes extract and its biomedical application, *IOP Conf. Ser.: Mater. Sci. Eng.*, 2020, **881**, 1–9.
- 135 S. O. Aisida, N. Madubuonu, M. H. Alnasir, I. Ahmad, S. Botha, M. Maaza and F. I. Ezema, Biogenic synthesis of iron oxide nanorods using Moringa oleifera leaf extract for antibacterial applications, *Appl. Nanosci.*, 2020, **10**, 305–315.
- 136 S. Qasim, A. Zafar, M. S. Saif, Z. Ali, M. Nazar, M. Waqas, A. U. Haq, T. Tariq, S. G. Hassan, F. Iqbal, X.-G. Shu and M. Hasan, Green synthesis of iron oxide nanorods using Withania coagulans extract improved photocatalytic degradation and antimicrobial activity, *J. Photochem. Photobiol. B, Biol.*, 2020, **204**, 111784.
- 137 F. Farouk, M. Abdelmageed, M. Azam Ansari and H. M. E. Azzazy, Synthesis of magnetic iron oxide nanoparticles using pulp and seed aqueous extract of Citrullus colocynth and evaluation of their antimicrobial activity, *Biotechnol. Lett.*, 2020, **42**, 231–240.
- 138 L. P. Yan, S. C. B. Gopinath, P. Anbu, F. H. Kasim, H. I. Zulhaimi and A. R. W. Yaakub, Characterization and anti-bacterial potential of iron oxide nanoparticle processed eco-friendly by plant extract, *Prep. Biochem. Biotechnol.*, 2020, **50**, 1053–1062.
- 139 J. Sandhya and S. Kalaiselvam, Biogenic synthesis of magnetic iron oxide nanoparticles using inedible borassus flabellifer seed coat: characterization, antimicrobial, antioxidant activity and *in vitro* cytotoxicity analysis, *Mater. Res. Express*, 2020, **7**, 015045.
- 140 M. Bashir, S. Ali and M. A. Farrukh, Green Synthesis of Fe<sub>2</sub>O<sub>3</sub> Nanoparticles from Orange Peel Extract and a Study of Its Antibacterial Activity, *J. Korean Phys. Soc.*, 2020, **76**, 848–854.
- 141 F. Erci and R. Cakir-Koc, Rapid green synthesis of noncytotoxic iron oxide nanoparticles using aqueous leaf extract of Thymbra spicata and evaluation of their antibacterial, antibiofilm, and antioxidant activity, *Inorg. Nano-Met. Chem.*, 2021, **51**, 683–692.
- 142 A. Rajendran, M. Alsawalha and T. Alomayri, Biogenic synthesis of husked rice-shaped iron oxide nanoparticles using coconut pulp (Cocos nucifera L.) extract for photocatalytic degradation of Rhodamine B dye and their *in vitro* antibacterial and anticancer activity, *J. Saudi Chem. Soc.*, 2021, **25**, 101307.
- 143 W. Ahmad, K. Kumar Jaiswal and M. Amjad, Euphorbia herita leaf extract as a reducing agent in a facile green synthesis of iron oxide nanoparticles and antimicrobial activity evaluation, *Inorg. Nano-Met. Chem.*, 2021, **51**, 1147–1154.
- 144 R. Periakaruppan, X. Chen, K. Thangaraj, A. Jeyaraj, H. H. Nguyen, Y. Yu, S. Hu, L. Lu and X. Li, Utilization of tea resources with the production of superparamagnetic biogenic iron oxide nanoparticles and an assessment of their antioxidant activities, *J. Cleaner Prod.*, 2021, **278**, 123962.
- 145 A. Jalal and N. Fakhre, *Preparation and Characterization of Green Fe<sub>3</sub>O<sub>4</sub> Nanoparticle Using the Aqueous Plant Extract of Gundelia Tournefortii L*, Aro-The Scientific Journal of Koya University, 2021, vol. 9, pp. 58–63.
- 146 M. Sriramulu, Balaji and S. Sumathi, Photo Catalytic, Antimicrobial and Antifungal Activity of Biogenic Iron Oxide Nanoparticles Synthesised Using *Aegle marmelos* Extracts, *J. Inorg. Organomet. Polym.*, 2021, **31**, 1738–1744.
- 147 M. W. Yaseen, M. Sufyan, R. Nazir, A. Naseem, R. Shah, A. A. Sheikh and M. Iqbal, Simple and cost-effective approach to synthesis of iron magnesium oxide nanoparticles using *Alstonia scholaris* and *Polyalthia*



- longifolia* leaves extracts and their antimicrobial, antioxidant and larvicidal activities, *Appl. Nanosci.*, 2021, **11**, 2479–2488.
- 148 Y. P. Teoh, Z. X. Ooi, S. S. Leong, P. T. Ng and W. W. Liu, Green Synthesis of Iron Oxide Nanoparticle Using Coffee Seed Extract and Its Antibacterial Activity, *J. Eng. Sci.*, 2021, **17**, 19–29.
- 149 Ö. Erdoğan, S. Paşa, G. M. Demirbolat and O. Çevik, Green biosynthesis, characterization, and cytotoxic effect of magnetic iron nanoparticles using Brassica Oleracea var capitata sub var rubra (red cabbage) aqueous peel extract, *Turk. J. Chem.*, 2021, **45**, 1086–1096.
- 150 P. N. Kirdat, P. B. Dandge, R. M. Hagwane, A. S. Nikam, S. P. Mahadik and S. T. Jirange, Synthesis and characterization of ginger (*Z. officinale*) extract mediated iron oxide nanoparticles and its antibacterial activity, *Mater. Today: Proc.*, 2021, **43**, 2826–2831.
- 151 A. Bouafia, S. E. Laouini, A. Khelef, M. L. Tedjani and F. Guemari, Effect of Ferric Chloride Concentration on the Type of Magnetite ( $\text{Fe}_3\text{O}_4$ ) Nanoparticles Biosynthesized by Aqueous Leaves Extract of Artemisia and Assessment of Their Antioxidant Activities, *J. Cluster Sci.*, 2021, **32**, 1033–1041.
- 152 M. Yusefi, K. Shameli, O. S. Yee, S.-Y. Teow, Z. Hedayatnasab, H. Jahangirian, T. J. Webster and K. Kuća, Green synthesis of  $\text{Fe}_3\text{O}_4$  nanoparticles stabilized by a Garcinia mangostana fruit peel extract for hyperthermia and anticancer activities, *Int. J. Nanomed.*, 2021, **16**, 2515.
- 153 L. Shaker Ardakani, V. Alimardani, A. M. Tamaddon, A. M. Amani and S. Taghizadeh, Green synthesis of iron-based nanoparticles using Chlorophytum comosum leaf extract: methyl orange dye degradation and antimicrobial properties, *Heliyon*, 2021, **7**, e06159.
- 154 A. Biswas, C. Vanlalveni, R. Lalfakzuala, S. Nath and L. Rokhum, Mikania mikrantha leaf extract mediated biogenic synthesis of magnetic iron oxide nanoparticles: Characterization and its antimicrobial activity study, *Mater. Today: Proc.*, 2021, **42**, 1366–1373.
- 155 M. A. Abid, D. A. Abid, W. J. Aziz and T. M. Rashid, Iron oxide nanoparticles synthesized using garlic and onion peel extracts rapidly degrade methylene blue dye, *Physica B Condens. Matter.*, 2021, **622**, 413277.
- 156 E. Üstün, S. C. Önbaş, S. K. Çelik, M. C. Ayvaz and N. Şahin, Green synthesis of iron oxide nanoparticles by using Ficus carica leaf extract and its antioxidant activity, *Biointerface Res. Appl. Chem.*, 2022, **2021**, 2108–2116.
- 157 K. Velsankar, G. Parvathy, S. Mohandoss, M. Krishna Kumar and S. Sudhakar, Celosia argentea leaf extract-mediated green synthesized iron oxide nanoparticles for bio-applications, *J. Nanostructure Chem.*, 2022, **12**, 625–640.
- 158 M. S. Haydar, D. Das, S. Ghosh and P. Mandal, Implementation of mature tea leaves extract in bioinspired synthesis of iron oxide nanoparticles: preparation, process optimization, characterization, and assessment of therapeutic potential, *Chem. Pap.*, 2022, **76**, 491–514.
- 159 S. Abd Al-hameed and A. M. Mohammed, Novel green synthesis of  $\text{Fe}_2\text{O}_3$  nanoparticles using persimmon extract and study their anti-cancer and anti-bacterial activity, *J. Pharm. Negat. Results*, 2022, **13**, 958–967.
- 160 D. Mundekkad and A. V. Alex, Analysis of structural and biomimetic characteristics of the green-synthesized  $\text{Fe}_3\text{O}_4$  nanozyme from the fruit peel extract of Punica granatum, *Chem. Pap.*, 2022, **76**, 3863–3878.
- 161 F. A. Al-Zahrani, S. S. Salem, H. A. Al-Ghamdi, L. M. Nhari, L. Lin and R. M. El-Shishtawy, Green synthesis and antibacterial activity of  $\text{Ag}/\text{Fe}_2\text{O}_3$  nanocomposite using Buddleja lindleyana extract, *Bioengineering*, 2022, **9**, 452.
- 162 F. Buarki, H. AbuHassan, F. Al Hannan and F. Z. Henari, Green Synthesis of Iron Oxide Nanoparticles Using Hibiscus rosa sinensis Flowers and Their Antibacterial Activity, *J. Nanotechnol.*, 2022, **2022**, 5474645.
- 163 S. Kumar, S. Ashique, H. Kumar, S. Verma, K. Dutt, A. Goswami, S. Pal, D. S. Chopra, Sonali, A. Iqbal and I. Kayes, Green Synthesis and Evaluation of Quercetin Conjugated Superparamagnetic Iron Oxide Nanoparticles, *J. Harbin Inst. Technol.*, 2022, **54**, 53–61.
- 164 J. Xiu, Y. Zhang, B. A. Paray, A. Gulnaz and M. War, Facile preparation of  $\text{Fe}_2\text{O}_3$  nanoparticles mediated by Centaurea alba extract and assessment of the anti-atherosclerotic properties, *Arabian J. Chem.*, 2022, **15**, 103493.
- 165 Y. Shah, M. Maharana and S. Sen, Peltophorum pterocarpum leaf extract mediated green synthesis of novel iron oxide particles for application in photocatalytic and catalytic removal of organic pollutants, *Biomass Convers. Biorefin.*, 2022, 1–14.
- 166 N. Dildar, S. N. Ali, T. Sohail, M. Lateef, S. T. Khan, S. F. Bukhari and P. Fazil, Biosynthesis, Characterization, Radical Scavenging and Antimicrobial Properties of Psidium guajava Linn Coated Silver and Iron Oxide Nanoparticles, *Egypt. J. Chem.*, 2022, **65**, 145–151.
- 167 M. Rizvi, T. Bhatia and R. Gupta, Green & sustainable synthetic route of obtaining iron oxide nanoparticles using Hylocereus undantus (pitaya or dragon fruit), *Mater. Today: Proc.*, 2022, **50**, 1100–1106.
- 168 H. Al-Karagoly, A. Rhyaf, H. Naji, S. Albukhaty, F. A. AlMalki, A. A. Alyamani, J. Albaqami and S. Aloufi, Green synthesis, characterization, cytotoxicity, and antimicrobial activity of iron oxide nanoparticles using Nigella sativa seed extract, *Green Process. Synth.*, 2022, **11**, 254–265.
- 169 S. Khan, G. Bibi, S. Dilbar, A. Iqbal, M. Ahmad, A. Ali, Z. Ullah, M. Jaremko, J. Iqbal and M. Ali, Biosynthesis and characterization of iron oxide nanoparticles from Mentha spicata and screening its combating potential against Phytophthora infestans, *Front. Plant Sci.*, 2022, **13**, 1001499.
- 170 C. Sudhakar, M. Poonkothai, T. Selvankumar and K. Selvam, Facile synthesis of iron oxide nanoparticles using Cassia auriculata flower extract and accessing their photocatalytic degradation and larvicidal effect, *J. Mater. Sci. Mater. Electron.*, 2022, **33**, 11434–11445.



- 171 W. Muzafar, T. Kanwal, K. Rehman, S. Perveen, T. Jabri, F. Qamar, S. Faizi and M. R. Shah, Green synthesis of iron oxide nanoparticles using *Melia azedarach* flowers extract and evaluation of their antimicrobial and antioxidant activities, *J. Mol. Struct.*, 2022, **1269**, 133824.
- 172 K. Velsankar, G. Parvathy, S. Mohandoss, G. Ravi and S. Sudhahar, *Echinochloa frumentacea* grains extract mediated synthesis and characterization of iron oxide nanoparticles: A greener nano drug for potential biomedical applications, *J. Drug Delivery Sci. Technol.*, 2022, **76**, 103799.
- 173 R. R. Pillai, P. B. Sreelekshmi, A. P. Meera and S. Thomas, Biosynthesized iron oxide nanoparticles: Cytotoxic evaluation against human colorectal cancer cell lines, *Mater. Today: Proc.*, 2022, **50**, 187–195.
- 174 C. Harmansah, M. Karatay Kutman and F. Z. Biber Muftuler, Preparation of iron oxide nanoparticles by banana peels extract and its usage in NDT, *Measurement*, 2022, **204**, 112081.
- 175 I. Ashraf, N. B. Singh and A. Agarwal, Green synthesis of iron oxide nanoparticles using Amla seed for methylene blue dye removal from water, *Mater. Today: Proc.*, 2023, **72**, 311–316.
- 176 Z. Isik, R. Bouchareb, H. Arslan, S. Özdemir, S. Gonca, N. Dizge, D. Balakrishnan and S. V. S. Prasad, Green synthesis of iron oxide nanoparticles derived from water and methanol extract of *Centaurea solstitialis* leaves and tested for antimicrobial activity and dye decolorization capability, *Environ. Res.*, 2023, **219**, 115072.
- 177 K. Andrade-Zavaleta, Y. Chacon-Laiza, D. Asmat-Campos and N. Raquel-Checca, Green Synthesis of Superparamagnetic Iron Oxide Nanoparticles with *Eucalyptus globulus* Extract and Their Application in the Removal of Heavy Metals from Agricultural Soil, *Molecules*, 2022, **27**, 1367.
- 178 N. Hoffmann, G. Tortella, E. Hermosilla, P. Fincheira, M. C. Diez, I. M. Lourenço, A. B. Seabra and O. Rubilar, Comparative Toxicity Assessment of Eco-Friendly Synthesized Superparamagnetic Iron Oxide Nanoparticles (SPIONs) in Plants and Aquatic Model Organisms, *Minerals*, 2022, **12**, 451.
- 179 K. Singh, D. Sethi Chopra, D. Singh and N. Singh, Green synthesis and characterization of iron oxide nanoparticles using *Coriandrum sativum* L. leaf extract, *Indian J. Biochem. Biophys.*, 2022, **59**, 450–454.
- 180 J. C. Tarafdar and R. Raliya, Rapid, Low-Cost, and Ecofriendly Approach for Iron Nanoparticle Synthesis Using *Aspergillus oryzae* TFR9, *J. Nanopart.*, 2013, **2013**, 141274.
- 181 M. Guilger-Casagrande and R. D. Lima, Synthesis of Silver Nanoparticles Mediated by Fungi: A Review, *Front. Bioeng. Biotechnol.*, 2019, **7**, 287.
- 182 S. Chatterjee, S. Mahanty, P. Das, P. Chaudhuri and S. Das, Biofabrication of iron oxide nanoparticles using manglicolous fungus *Aspergillus niger* BSC-1 and removal of Cr(VI) from aqueous solution, *Chem. Eng. J.*, 2020, **385**, 123790.
- 183 T. J. Beveridge, M. N. Hughes, H. Lee, K. T. Leung, R. K. Poole, I. Savvaidis, S. Silver and J. T. Trevors, Metal-Microbe Interactions: Contemporary Approaches, *Adv. Microb. Physiol.*, 1997, **38**, 177–243.
- 184 M. Gericke and A. Pinches, Biological synthesis of metal nanoparticles, *Hydrometallurgy*, 2006, **83**, 132–140.
- 185 N. A. Wani, W. I. Khanday and S. Tirumale, Biosynthesis of iron oxide nanoparticles using ethyl acetate extract of *Chaetomium cupreum* and their anticancer activity, *Matrix Sci. Pharma*, 2021, **40**, 23–30.
- 186 S. Saqib, W. Zaman, A. Ayaz, S. Habib, S. Bahadur, S. Hussain, S. Muhammad and F. Ullah, Postharvest disease inhibition in fruit by synthesis and characterization of chitosan iron oxide nanoparticles, *Biocatal. Agric. Biotechnol.*, 2020, **28**, 101729.
- 187 A. Ali, N. Elewa, N. Elbostany, Y. Shetaia and M. Swilm, Antimicrobial potentiality of green synthesized iron oxide nanoparticles by *Penicillium roqueforti*, *Egypt J. Pure Appl. Sci.*, 2021, **59**, 29–43.
- 188 R. Safarkar, G. Ebrahimzadeh Rajaei and S. Khalili-Arjagi, The study of antibacterial properties of iron oxide nanoparticles synthesized using the extract of lichen *Ramalina sinensis*, *Asian J. Nanosci. Mater.*, 2020, **3**, 157–166.
- 189 G. Manik and R. Ramasubbu, Biosynthesis of Iron Nanoparticles from *Pleurotus florida* and its Antimicrobial Activity against Selected Human Pathogens, *Indian J. Pharm. Sci.*, 2021, **83**, 45–51.
- 190 H. Sayed, H. Sadek, M. Abdel-Aziz, N. Mahmoud, W. Sabry, G. Genidy and M. Maher, Biosynthesis of iron oxide nanoparticles from fungi isolated from deteriorated historical gilded cartonnage and its application in cleaning, *Egypt J. Archeol. Restor. Stud.*, 2021, **11**, 129–145.
- 191 N. Pantidos and L. E. Horsfall, Biological synthesis of metallic nanoparticles by bacteria, fungi and plants, *J. Nanomed. Nanotechnol.*, 2014, **5**, 1.
- 192 A. Fariq, T. Khan and A. Yasmin, Microbial synthesis of nanoparticles and their potential applications in biomedicine, *J. Appl. Biomed.*, 2017, **15**, 241–248.
- 193 G. Gahlawat and A. R. Choudhury, A review on the biosynthesis of metal and metal salt nanoparticles by microbes, *RSC Adv.*, 2019, **9**, 12944–12967.
- 194 P. Singh, Y.-J. Kim, D. Zhang and D.-C. Yang, Biological synthesis of nanoparticles from plants and microorganisms, *Trends Biotechnol.*, 2016, **34**, 588–599.
- 195 H. Alam, N. Khatoon, M. A. Khan, S. A. Husain, M. Saravanan and M. Sardar, Synthesis of selenium nanoparticles using probiotic bacteria *Lactobacillus acidophilus* and their enhanced antimicrobial activity against resistant bacteria, *J. Cluster Sci.*, 2020, **31**, 1003–1011.
- 196 A. S. Jubran, O. M. Al-Zamely and M. H. Al-Ammar, A study of iron oxide nanoparticles synthesis by using bacteria, *Int. J. Pharm. Qual. Assur.*, 2020, **11**, 1–8.
- 197 S. Majeed, M. Danish, M. N. Mohamad Ibrahim, S. H. Sekeri, M. T. Ansari, A. Nanda and G. Ahmad, Bacteria Mediated Synthesis of Iron Oxide Nanoparticles



- and Their Antibacterial, Antioxidant, Cytocompatibility Properties, *J. Cluster Sci.*, 2021, **32**, 1083–1094.
- 198 M. A. Ali and M. H. Alkhafaji, Antibiofilm Activity of Biosynthesized Enterococcus-Iron Oxide Nanoparticles against uropathogenic Bacteria, *Egypt. J. Bot.*, 2023, **63**, 1201–1214.
- 199 Q. A. Al-Maliki and W. R. Taj-Aldeen, Antibacterial Activity Of Bacterial Mediated Synthesized Iron Oxide Nanoparticles Using Bacillus Coagulans, *Nat. Volatiles Essent. Oils*, 2022, **9**, 1312–1320.
- 200 M. Kumar, G. Gupta, T. Varghese, A. M. Shankregowda, P. P. Srivastava, S. Bhushan, P. P. Shukla, G. Krishna and S. Gupta, Synthesis and characterisation of superparamagnetic iron oxide nanoparticles (SPIONs) for minimising Aeromonas hydrophila load from freshwater, *Curr. Nanosci.*, 2022, **18**, 224–236.
- 201 V. Subramaniam, S. R. Subashchandrabose, V. Ganeshkumar, P. Thavamani, Z. Chen, R. Naidu and M. Megharaj, Cultivation of Chlorella on brewery wastewater and nano-particle biosynthesis by its biomass, *Bioresour. Technol.*, 2016, **211**, 698–703.
- 202 H. Agarwal, S. V. Kumar and S. Rajeshkumar, A review on green synthesis of zinc oxide nanoparticles—An eco-friendly approach, *Resour.-Effic. Technol.*, 2017, **3**, 406–413.
- 203 K. S. Siddiqi and A. Husen, Fabrication of metal nanoparticles from fungi and metal salts: scope and application, *Nanoscale Res. Lett.*, 2016, **11**, 1–15.
- 204 D. M. Salem, M. M. Ismail and H. R. Tadros, Evaluation of the antibiofilm activity of three seaweed species and their biosynthesized iron oxide nanoparticles (Fe<sub>3</sub>O<sub>4</sub>-NPs), *Egypt. J. Aquat. Res.*, 2020, **46**, 333–339.
- 205 M. L. Budlayan, J. N. Patricio, S. D. Arco, R. Y. Capangpangan and A. C. Alguno, Effects of precursor concentration on the properties of magnetic iron oxide nanoparticles synthesized using brown seaweed (Sargassum crassifolium) extract, *Mater. Today: Proc.*, 2021, **46**, 1608–1612.
- 206 Z. Peng, Z. Fan, X. Chen, X. Zhou, Z. F. Gao, S. Deng, S. Wan, X. Lv, Y. Shi and W. Han, Fabrication of Nano Iron Oxide-Modified Biochar from Co-Hydrothermal Carbonization of Microalgae and Fe (II) Salt for Efficient Removal of Rhodamine B, *Nanomater*, 2022, **12**, 2271.
- 207 C. Yu, J. Tang, H. Su, J. Huang, F. Liu, L. Wang and H. Sun, Development of a novel biochar/iron oxide composite from green algae for bisphenol-A removal: Adsorption and Fenton-like reaction, *Environ. Technol. Innov.*, 2022, 102647.
- 208 G. Sarojini, S. Venkateshbabu and M. Rajasimman, Facile synthesis and characterization of polypyrrole-iron oxide-seaweed (PPy-Fe<sub>3</sub>O<sub>4</sub>-SW) nanocomposite and its exploration for adsorptive removal of Pb (II) from heavy metal bearing water, *Chemosphere*, 2021, **278**, 130400.
- 209 R. Selvaraj, G. Murugesan, G. Rangasamy, R. Bhole, N. Dave, S. Pai, K. Balakrishna, R. Vinayagam and T. Varadavenkatesan, As (III) removal using superparamagnetic magnetite nanoparticles synthesized using Ulva prolifera— optimization, isotherm, kinetic and equilibrium studies, *Chemosphere*, 2022, **308**, 136271.
- 210 S. O. Aisida, P. A. Akpa, I. Ahmad, M. Maaza and F. I. Ezema, Influence of PVA, PVP and PEG doping on the optical, structural, morphological and magnetic properties of zinc ferrite nanoparticles produced by thermal method, *Physica B Condens. Matter*, 2019, **571**, 130–136.
- 211 D. O. Okoroh, J. Ozuomba, S. O. Aisida and P. U. Asogwa, Thermal treated synthesis and characterization of polyethylene glycol (PEG) mediated zinc ferrite nanoparticles, *Surf. Interfaces*, 2019, **16**, 127–131.
- 212 D. O. Okoroh, J. O. Ozuomba, S. O. Aisida and P. U. Asogwa, Properties of zinc ferrite nanoparticles due to PVP mediation and annealing at 500 °C, *Adv. Nanopart.*, 2019, **8**, 36–45.
- 213 M. Chastellain, A. Petri, A. Gupta, K. V. Rao and H. Hofmann, Superparamagnetic silica-iron oxide nanocomposites for application in hyperthermia, *Adv. Eng. Mater.*, 2004, **6**, 235–241.
- 214 R. Weissleder, D. D. Stark, B. L. Engelstad, B. R. Bacon, C. C. Compton, D. L. White, P. Jacobs and J. Lewis, Superparamagnetic iron oxide: pharmacokinetics and toxicity, *Am. J. Roentgenol.*, 1989, **152**, 167–173.
- 215 S. M. Dadfar, K. Roemhild, N. I. Drude, S. Von Stillfried, R. Knüchel, F. Kiessling and T. Lammers, Iron oxide nanoparticles: Diagnostic, therapeutic and theranostic applications, *Adv. Drug Delivery Rev.*, 2019, **138**, 302–325.
- 216 R. P. Dhavale, S. B. Parit, S. C. Sahoo, P. Kollu, P. S. Patil, P. B. Patil and A. D. Chougale,  $\alpha$ -amylase immobilized on magnetic nanoparticles: reusable robust nano-biocatalyst for starch hydrolysis, *Mater. Res. Express*, 2018, **5**, 075403.
- 217 N. Madubuonu, S. O. Aisida, A. Ali, I. Ahmad, T.-K. Zhao, S. Botha, M. Maaza and F. I. Ezema, Biosynthesis of iron oxide nanoparticles via a composite of Psidium guajava-Moringa oleifera and their antibacterial and photocatalytic study, *J. Photochem. Photobiol. B, Biol.*, 2019, **199**, 111601.
- 218 Y. Zhang, M. Liu, Y. Zhang, X. Chen, W. Ren and Z.-G. Ye, Atomic layer deposition of superparamagnetic and ferrimagnetic magnetite thin films, *J. Appl. Phys.*, 2015, **117**, 17C743.
- 219 M. G. Naseri, E. B. Saion, M. Hashim, A. H. Shaari and H. A. Ahangar, Synthesis and characterization of zinc ferrite nanoparticles by a thermal treatment method, *Solid State Commun.*, 2011, **151**, 1031–1035.
- 220 S. Arora, Superparamagnetic iron oxide nanoparticles: magnetic nanoplatforms as drug carriers, *Int. J. Nanomed.*, 2012, **7**, 3445.
- 221 H. Mok and M. Zhang, Superparamagnetic iron oxide nanoparticle-based delivery systems for biotherapeutics, *Expert Opin. Drug Delivery*, 2013, **10**, 73–87.
- 222 C. S. Hurlbut and C. Klein, *Manual of Mineralogy*, ed. J. D. Dana, Wiley, New York, 1993.
- 223 G. H. Kwei, R. B. Von Dreele, A. Williams, J. A. Goldstone, A. C. Lawson and W. K. Warburton, Structure and valence from complementary anomalous X-ray and neutron powder diffraction, *J. Mol. Struct.*, 1990, **223**, 383–406.



- 224 S. Naqvi, M. Samim, A. Abdin, F. J. Ahmed, A. Maitra, C. Prashant and A. K. Dinda, Concentration-dependent toxicity of iron oxide nanoparticles mediated by increased oxidative stress, *Int. J. Nanomed.*, 2010, **5**, 983.
- 225 Z. Sun, V. Yathindranath, M. Worden, J. A. Thliveris, S. Chu, F. E. Parkinson, T. Hegmann and D. W. Miller, Characterization of cellular uptake and toxicity of aminosilane-coated iron oxide nanoparticles with different charges in central nervous system-relevant cell culture models, *Int. J. Nanomed.*, 2013, **8**, 961–970.
- 226 Z. M. Saiyed, N. H. Gandhi and M. P. Nair, Magnetic nanoformulation of azidothymidine 5'-triphosphate for targeted delivery across the blood-brain barrier, *Int. J. Nanomed.*, 2010, **5**, 157–166.
- 227 M. Arruebo, R. Fernández-Pacheco, M. R. Ibarra and J. Santamaría, Magnetic nanoparticles for drug delivery, *Nano Today*, 2007, **2**, 22–32.
- 228 J. Gao, H. Gu and B. Xu, Multifunctional magnetic nanoparticles: design, synthesis, and biomedical applications, *Acc. Chem. Res.*, 2009, **42**, 1097–1107.
- 229 G. Prabha and V. Raj, Preparation and characterization of polymer nanocomposites coated magnetic nanoparticles for drug delivery applications, *J. Magn. Magn. Mater.*, 2016, **408**, 26–34.
- 230 J. Xu, J. Sun, Y. Wang, J. Sheng, F. Wang and M. Sun, Application of iron magnetic nanoparticles in protein immobilization, *Molecules*, 2014, **19**, 11465–11486.
- 231 T. K. Jain, M. K. Reddy, M. A. Morales, D. L. Leslie-Pelecky and V. Labhasetwar, Biodistribution, Clearance, and Biocompatibility of Iron Oxide Magnetic Nanoparticles in Rats, *Mol. Pharm.*, 2008, **5**, 316–327.
- 232 W. Wu, Q. He and C. Jiang, Magnetic Iron Oxide Nanoparticles: Synthesis and Surface Functionalization Strategies, *Nanoscale Res. Lett.*, 2008, **3**, 397.
- 233 A. Andrade, D. Souza, M. Pereira, J. Fabris and R. Domingues, Synthesis and characterization of magnetic nanoparticles coated with silica through a sol-gel approach, *Ceramica*, 2009, **55**, 420–424.
- 234 S. O. Aisida, P. A. Akpa, I. Ahmad, T.-K. Zhao, M. Maaza and F. I. Ezema, Bio-inspired encapsulation and functionalization of iron oxide nanoparticles for biomedical applications, *Eur. Polym. J.*, 2020, **122**, 109371.
- 235 Z. Chen, H. Ji, C. Liu, W. Bing, Z. Wang and X. Qu, A Multinuclear Metal Complex Based DNase-Mimetic Artificial Enzyme: Matrix Cleavage for Combating Bacterial Biofilms, *Angew Chem. Int. Ed. Engl.*, 2016, **55**, 10732–10736.
- 236 K. Korschelt, R. Ragg, C. S. Metzger, M. Kluncker, M. Oster, B. Barton, M. Panthöfer, D. Strand, U. Kolb, M. Mondeshki, S. Strand, J. Brieger, M. N. Tahir and W. Tremel, Glycine-functionalized copper(ii) hydroxide nanoparticles with high intrinsic superoxide dismutase activity, *Nanoscale*, 2017, **9**, 3952–3960.
- 237 A. Sun, L. Mu and X. Hu, Graphene Oxide Quantum Dots as Novel Nanozymes for Alcohol Intoxication, *ACS Appl. Mater. Interfaces*, 2017, **9**, 12241–12252.
- 238 L. Gao, K. Fan and X. Yan, Iron Oxide Nanozyme: A Multifunctional Enzyme Mimetic for Biomedical Applications, *Theranostics*, 2017, **7**, 3207–3227.
- 239 Y. Song, K. Qu, C. Zhao, J. Ren and X. Qu, Graphene Oxide: Intrinsic Peroxidase Catalytic Activity and Its Application to Glucose Detection, *Adv. Mater.*, 2010, **22**, 2206–2210.
- 240 R. Ragg, M. N. Tahir and W. Tremel, Solids Go Bio: Inorganic Nanoparticles as Enzyme Mimics, *Eur. J. Inorg. Chem.*, 2016, **2016**, 1906–1915.
- 241 H. Cheng, S. Lin, F. Muhammad, Y.-W. Lin and H. Wei, Rationally Modulate the Oxidase-like Activity of Nanoceria for Self-Regulated Bioassays, *ACS Sens.*, 2016, **1**, 1336–1343.
- 242 S. Singh, Cerium oxide based nanozymes: Redox phenomenon at biointerfaces, *Biointerphases*, 2016, **11**, 04b202.
- 243 Z. Dong, Q. Luo and J. Liu, Artificial enzymes based on supramolecular scaffolds, *Chem. Soc. Rev.*, 2012, **41**, 7890–7908.
- 244 Z. Shen, A. Wu and X. Chen, Iron Oxide Nanoparticle Based Contrast Agents for Magnetic Resonance Imaging, *Mol. Pharm.*, 2017, **14**, 1352–1364.
- 245 N. Lee, D. Yoo, D. Ling, M. H. Cho, T. Hyeon and J. Cheon, Iron Oxide Based Nanoparticles for Multimodal Imaging and Magneto-responsive Therapy, *Chem. Rev.*, 2015, **115**, 10637–10689.
- 246 G. Liu, J. Gao, H. Ai and X. Chen, Applications and potential toxicity of magnetic iron oxide nanoparticles, *Small*, 2013, **9**, 1533–1545.
- 247 V. Naresh and N. Lee, A Review on Biosensors and Recent Development of Nanostructured Materials-Enabled Biosensors, *Sensors*, 2021, **21**, 1109.
- 248 R. G. Mahmudunnabi, F. Farhana, N. Kashaninejad, S. Firoz, Y.-B. Shim and M. Shiddiky, Nanozyme-based electrochemical biosensors for disease biomarker detection, *Analyst*, 2020, **145**, 4398–4420.
- 249 L. Gao, K. Fan and X. Yan, Iron Oxide Nanozyme: A Multifunctional Enzyme Mimetic for Biomedical Applications, *Theranostics*, 2017, **7**, 3207–3227.
- 250 L. Gao, J. Zhuang, L. Nie, J. Zhang, Y. Zhang, N. Gu, T. Wang, J. Feng, D. Yang, S. Perrett and X. Yan, Intrinsic peroxidase-like activity of ferromagnetic nanoparticles, *Nat. Nanotechnol.*, 2007, **2**, 577–583.
- 251 D. P. Cormode, L. Gao and H. Koo, Emerging Biomedical Applications of Enzyme-Like Catalytic Nanomaterials, *Trends Biotechnol.*, 2018, **36**, 15–29.
- 252 J. Hernández-Ruiz, M. Arnao, A. Hiner, G. Canovas and M. Acosta, Catalase-like activity of horseradish peroxidase: Relationship to enzyme inactivation by H<sub>2</sub>O<sub>2</sub>, *J. Biol. Chem.*, 2001, **354**, 107–114.
- 253 P. Campomanes, U. Rothlisberger, M. Alfonso-Prieto and C. Rovira, The Molecular Mechanism of the Catalase-like Activity in Horseradish Peroxidase, *J. Am. Chem. Soc.*, 2015, **137**, 11170–11178.
- 254 G. F. Goya, A. Mayoral, E. Winkler, R. D. Zysler, C. Bagnato, M. Raineri, J. A. Fuentes-García and E. Lima, Next generation of nanozymes: A perspective of the challenges



- to match biological performance, *J. Appl. Phys.*, 2021, **130**, 190903.
- 255 R. Zhang, L. Chen, Q. Liang, J. Xi, H. Zhao, Y. Jin, X. Gao, X. Yan, L. Gao and K. Fan, Unveiling the active sites on ferrihydrite with apparent catalase-like activity for potentiating radiotherapy, *Nano Today*, 2021, **41**, 101317.
- 256 B. Das, J. L. Franco, N. Logan, P. Balasubramanian, M. I. Kim and C. Cao, Nanozymes in Point-of-Care Diagnosis: An Emerging Futuristic Approach for Biosensing, *Nano-Micro Lett.*, 2021, **13**, 1–51.
- 257 X. Ren, D. Chen, Y. Wang, H. Li, Y. Zhang, H. Chen, X. Li and M. Huo, Nanozymes-recent development and biomedical applications, *J. Nanobiotechnol.*, 2022, **20**, 92.
- 258 A. Dutta, S. Maji, D. Srivastava, A. Mondal, P. Biswas, P. Paul and B. Adhikary, Peroxidase-like activity and amperometric sensing of hydrogen peroxide by Fe<sub>2</sub>O<sub>3</sub> and Prussian Blue-modified Fe<sub>2</sub>O<sub>3</sub> nanoparticles, *J. Mol. Catal. A: Chem.*, 2012, **360**, 71–77.
- 259 Z. Chen, J.-J. Yin, Y.-T. Zhou, Y. Zhang, L. Song, M. Song, S. Hu and N. Gu, Dual Enzyme-like Activities of Iron Oxide Nanoparticles and Their Implication for Diminishing Cytotoxicity, *ACS Nano*, 2012, **6**, 4001–4012.
- 260 M. Kurz and R. R. Breaker, In vitro selection of nucleic acid enzymes, *Curr. Top. Microbiol. Immunol.*, 1999, **243**, 137–158.
- 261 B. Liu, X. Han and J. Liu, Iron oxide nanozyme catalyzed synthesis of fluorescent polydopamine for light-up Zn<sup>2+</sup> detection, *Nanoscale*, 2016, **8**, 13620–13626.
- 262 R. Zhang, S. He, C. Zhang and W. Chen, Three-dimensional Fe- and N-incorporated carbon structures as peroxidase mimics for fluorescence detection of hydrogen peroxide and glucose, *J. Mater. Chem. B*, 2015, **3**, 4146–4154.
- 263 Y. Shi, P. Su, Y. Wang and Y. Yang, Fe<sub>3</sub>O<sub>4</sub> peroxidase mimetics as a general strategy for the fluorescent detection of H<sub>2</sub>O<sub>2</sub>-involved systems, *Talanta*, 2014, **130**, 259–264.
- 264 L. Gao, K. M. Giglio, J. L. Nelson, H. Sondermann and A. J. Travis, Ferromagnetic nanoparticles with peroxidase-like activity enhance the cleavage of biological macromolecules for biofilm elimination, *Nanoscale*, 2014, **6**, 2588–2593.
- 265 J. Qian, X. Yang, L. Jiang, C. Zhu, H. Mao and K. Wang, Facile preparation of Fe<sub>3</sub>O<sub>4</sub> nanospheres/reduced graphene oxide nanocomposites with high peroxidase-like activity for sensitive and selective colorimetric detection of acetylcholine, *Sens. Actuators, B*, 2014, **201**, 160–166.
- 266 Y. Lin, Y. Huang, J. Ren and X. Qu, Incorporating ATP into biomimetic catalysts for realizing exceptional enzymatic performance over a broad temperature range, *NPG Asia Mater.*, 2014, **6**, e114.
- 267 Y.-C. Yang, Y.-T. Wang and W.-L. Tseng, Amplified Peroxidase-Like Activity in Iron Oxide Nanoparticles Using Adenosine Monophosphate: Application to Urinary Protein Sensing, *ACS Appl. Mater. Interfaces*, 2017, **9**, 10069–10077.
- 268 N. V. S. Vallabani, A. S. Karakoti and S. Singh, ATP-mediated intrinsic peroxidase-like activity of Fe<sub>3</sub>O<sub>4</sub>-based nanozyme: One step detection of blood glucose at physiological pH, *Colloids Surf., B*, 2017, **153**, 52–60.
- 269 B. Liu and J. Liu, Accelerating peroxidase mimicking nanozymes using DNA, *Nanoscale*, 2015, **7**, 13831–13835.
- 270 C.-H. Liu, C.-J. Yu and W.-L. Tseng, Fluorescence assay of catecholamines based on the inhibition of peroxidase-like activity of magnetite nanoparticles, *Anal. Chim. Acta*, 2012, **745**, 143–148.
- 271 Y. S. Kim and J. Jurng, A simple colorimetric assay for the detection of metal ions based on the peroxidase-like activity of magnetic nanoparticles, *Sens. Actuators, B*, 2013, **176**, 253–257.
- 272 F. Yu, Y. Huang, A. J. Cole and V. C. Yang, The artificial peroxidase activity of magnetic iron oxide nanoparticles and its application to glucose detection, *Biomaterials*, 2009, **30**, 4716–4722.
- 273 N. V. S. Vallabani, A. S. Karakoti and S. Singh, ATP-mediated intrinsic peroxidase-like activity of Fe<sub>3</sub>O<sub>4</sub>-based nanozyme: One step detection of blood glucose at physiological Ph, *Colloids Surf., B*, 2017, **153**, 52–60.
- 274 Y. Song, X. Xia, X. Wu, P. Wang and L. Qin, Integration of Platinum Nanoparticles with a Volumetric Bar-Chart Chip for Biomarker Assays, *Angew. Chem., Int. Ed.*, 2014, **53**, 12451–12455.
- 275 K. Fan, H. Wang, J. Xi, Q. Liu, X. Meng, D. Duan, L. Gao and X. Yan, Optimization of Fe<sub>3</sub>O<sub>4</sub> nanozyme activity via single amino acid modification mimicking an enzyme active site, *Chem. Commun.*, 2017, **53**, 424–427.
- 276 N. Wang, L. Zhu, D. Wang, M. Wang, Z. Lin and H. Tang, Sono-assisted preparation of highly-efficient peroxidase-like Fe<sub>3</sub>O<sub>4</sub> magnetic nanoparticles for catalytic removal of organic pollutants with H<sub>2</sub>O<sub>2</sub>, *Ultrason. Sonochem.*, 2010, **17**, 526–533.
- 277 N. C. Veitch, Horseradish peroxidase: a modern view of a classic enzyme, *Phytochemistry*, 2004, **65**, 249–259.
- 278 X. Li and J. Paier, Adsorption of Water on the Fe<sub>3</sub>O<sub>4</sub> (111) Surface: Structures, Stabilities, and Vibrational Properties Studied by Density Functional Theory, *J. Phys. Chem. C*, 2016, **120**, 1056–1065.
- 279 S. Liu, F. Lu, R. Xing and J.-J. Zhu, Structural Effects of Fe<sub>3</sub>O<sub>4</sub> Nanocrystals on Peroxidase-Like Activity, *Chem.–Eur. J.*, 2011, **17**, 620–625.
- 280 H. Wei and E. Wang, Fe<sub>3</sub>O<sub>4</sub> Magnetic Nanoparticles as Peroxidase Mimetics and Their Applications in H<sub>2</sub>O<sub>2</sub> and Glucose Detection, *Anal. Chem.*, 2008, **80**, 2250–2254.
- 281 L. Gao, J. Wu, S. Lyle, K. Zehr, L. Cao and D. Gao, Magnetite Nanoparticle-Linked Immunosorbent Assay, *J. Phys. Chem. C*, 2008, **112**, 17357–17361.
- 282 X. Wang, R. Niessner, D. Tang and D. Knopp, Nanoparticle-based immunosensors and immunoassays for aflatoxins, *Anal. Chim. Acta*, 2016, **912**, 10–23.
- 283 D. Bhattacharya, A. Bakshi, I. Banerjee, R. Ananthkrishnan, T. K. Maiti and P. Pramanik, Development of phosphonate modified Fe<sub>(1-x)</sub>Mn<sub>x</sub>Fe<sub>2</sub>O<sub>4</sub> mixed ferrite nanoparticles: Novel peroxidase mimetics in enzyme linked immunosorbent assay, *Talanta*, 2011, **86**, 337–348.



- 284 M. Yang, Y. Guan, Y. Yang, L. Xie, T. Xia, W. Xiong and C. Guo, Immunological detection of hepatocellular carcinoma biomarker GP73 based on dissolved magnetic nanoparticles, *Colloids Surf., A*, 2014, **443**, 280–285.
- 285 M. Yang, Y. Guan, Y. Yang, T. Xia, W. Xiong, N. Wang and C. Guo, Peroxidase-like activity of amino-functionalized magnetic nanoparticles and their applications in immunoassay, *J. Colloid Interface Sci.*, 2013, **405**, 291–295.
- 286 M. Yang, Y. Guan, Y. Yang, T. Xia, W. Xiong and C. Guo, A sensitive and rapid immunoassay for mycoplasma pneumonia based on Fe<sub>3</sub>O<sub>4</sub> nanoparticles, *Mater. Lett.*, 2014, **137**, 113–116.
- 287 M. A. Woo, M. I. Kim, J. H. Jung, K. S. Park, T. S. Seo and H. G. Park, A novel colorimetric immunoassay utilizing the peroxidase mimicking activity of magnetic nanoparticles, *Int. J. Mol. Sci.*, 2013, **14**, 9999–10014.
- 288 M. I. Kim, M. S. Kim, M. A. Woo, Y. Ye, K. S. Kang, J. Lee and H. G. Park, Highly efficient colorimetric detection of target cancer cells utilizing superior catalytic activity of graphene oxide-magnetic-platinum nanohybrids, *Nanoscale*, 2014, **6**, 1529–1536.
- 289 Y. Wu, M. Song, Z. Xin, X. Zhang, Y. Zhang, C. Wang, S. Li and N. Gu, Ultra-small particles of iron oxide as peroxidase for immunohistochemical detection, *Nanotechnol.*, 2011, **22**, 225703.
- 290 D. Duan, K. Fan, D. Zhang, S. Tan, M. Liang, Y. Liu, J. Zhang, P. Zhang, W. Liu, X. Qiu, G. P. Kobinger, G. F. Gao and X. Yan, Nanozyme-strip for rapid local diagnosis of Ebola, *Biosens. Bioelectron.*, 2015, **74**, 134–141.
- 291 R. Thiramanas, K. Jangpatarapongsa, P. Tangboriboonrat and D. Polpanich, Detection of *Vibrio cholerae* using the intrinsic catalytic activity of a magnetic polymeric nanoparticle, *Anal. Chem.*, 2013, **85**, 5996–6002.
- 292 Z. Zhang, Z. Wang, X. Wang and X. Yang, Magnetic nanoparticle-linked colorimetric aptasensor for the detection of thrombin, *Sens. Actuators, B*, 2010, **147**, 428–433.
- 293 L. Wu, M. Zhou, Y. Wang and J. Liu, Nanozyme and aptamer-based immunosorbent assay for aflatoxin B1, *J. Hazard. Mater.*, 2020, **399**, 123154.
- 294 K. Fan, C. Cao, Y. Pan, D. Lu, D. Yang, J. Feng, L. Song, M. Liang and X. Yan, Magnetoferritin nanoparticles for targeting and visualizing tumour tissues, *Nat. Nanotechnol.*, 2012, **7**, 459–464.
- 295 J. Zhuang, K. Fan, L. Gao, D. Lu, J. Feng, D. Yang, N. Gu, Y. Zhang, M. Liang and X. Yan, Ex Vivo Detection of Iron Oxide Magnetic Nanoparticles in Mice Using Their Intrinsic Peroxidase-Mimicking Activity, *Mol. Pharm.*, 2012, **9**, 1983–1989.
- 296 D. Zhang, Y.-X. Zhao, Y.-J. Gao, F.-P. Gao, Y.-S. Fan, X.-J. Li, Z.-Y. Duan and H. Wang, Anti-bacterial and *in vivo* tumor treatment by reactive oxygen species generated by magnetic nanoparticles, *J. Mater. Chem. B*, 2013, **1**, 5100–5107.
- 297 K. Fan, C. Cao, Y. Pan, D. Lu, D. Yang, J. Feng, L. Song, M. Liang and X. Yan, Magnetoferritin nanoparticles for targeting and visualizing tumour tissues, *Nat. Nanotechnol.*, 2012, **7**, 459–464.
- 298 Y. Liu, P. Naha, G. Hwang, D. Kim, Y. Huang, A. Simon-Soro, H.-I. Jung, Z. Ren, Y. Li, S. Gubara, F. Alawi, D. Zero, A. T. Hara, D. P. Cormode and H. Koo, Topical ferumoxytol nanoparticles disrupt biofilms and prevent severe tooth decay *in vivo* via intrinsic catalytic activity, *Nat. Commun.*, 2018, **9**, 2920.
- 299 M. Huo, L. Wang, Y. Chen and J. Shi, Tumor-selective catalytic nanomedicine by nanocatalyst delivery, *Nat. Commun.*, 2017, **8**, 357.
- 300 S. E. Kim, L. Zhang, K. Ma, M. Riegman, F. Chen, I. Ingold, M. Conrad, M. Z. Turker, M. Gao, X. Jiang, S. Monette, M. Pauliah, M. Gonen, P. Zanzonico, T. Quinn, U. Wiesner, M. S. Bradbury and M. Overholtzer, Ultrasmall nanoparticles induce ferroptosis in nutrient-deprived cancer cells and suppress tumour growth, *Nat. Nanotechnol.*, 2016, **11**, 977–985.
- 301 S. Zanganeh, G. Hutter, R. Spitler, O. Lenkov, M. Mahmoudi, A. Shaw, J. S. Pajarinen, H. Nejadnik, S. Goodman, S. Moseley, L. M. Coussens and H. E. Daldrup-Link, Iron oxide nanoparticles inhibit tumour growth by inducing pro-inflammatory macrophage polarization in tumour tissues, *Nat. Nanotechnol.*, 2016, **11**, 986–994.
- 302 G. Tang, J. He, J. Liu, X. Yan and K. Fan, Nanozyme for tumor therapy: Surface modification matters, *Exploration*, 2021, **1**, 75–89.
- 303 F. Wei, X. Cui, Z. Wang, C. Dong, J. Li and X. Han, Recoverable peroxidase-like Fe<sub>3</sub>O<sub>4</sub>@MoS<sub>2</sub>-Ag nanozyme with enhanced antibacterial ability, *Chem. Eng. J.*, 2021, **408**, 127240.
- 304 Y. Wang, H. Li, L. Guo, Q. Jiang and F. Liu, A cobalt-doped iron oxide nanozyme as a highly active peroxidase for renal tumor catalytic therapy, *RSC Adv.*, 2019, **9**, 18815–18822.
- 305 K. Sun, Z. Gao, Y. Zhang, H. Wu, C. You, S. Wang, P. An, C. Sun and B. Sun, Enhanced highly toxic reactive oxygen species levels from iron oxide core-shell mesoporous silica nanocarrier-mediated Fenton reactions for cancer therapy, *J. Mater. Chem. B*, 2018, **6**, 5876–5887.
- 306 S. Li, L. Shang, B. Xu, S. Wang, K. Gu, Q. Wu, Y. Sun, Q. Zhang, H. Yang, F. Zhang, L. Gu, T. Zhang and H. Liu, A Nanozyme with Photo-Enhanced Dual Enzyme-Like Activities for Deep Pancreatic Cancer Therapy, *Angew. Chem., Int. Ed.*, 2019, **58**, 12624–12631.
- 307 N. V. S. Vallabani, A. Vinu, S. Singh and A. Karakoti, Tuning the ATP-triggered pro-oxidant activity of iron oxide-based nanozyme towards an efficient antibacterial strategy, *J. Colloid Interface Sci.*, 2020, **567**, 154–164.
- 308 H. Cheng, L. Zhang, J. He, W. Guo, Z. Zhou, X. Zhang, S. Nie and H. Wei, Integrated Nanozymes with Nanoscale Proximity for *in Vivo* Neurochemical Monitoring in Living Brains, *Anal. Chem.*, 2016, **88**, 5489–5497.
- 309 H. Wei and E. Wang, Fe<sub>3</sub>O<sub>4</sub> magnetic nanoparticles as peroxidase mimetics and their applications in H<sub>2</sub>O<sub>2</sub> and glucose detection, *Anal. Chem.*, 2008, **80**, 2250–2254.



- 310 Y. Gao, G. Wang, H. Huang, J. Hu, S. M. Shah and X. Su, Fluorometric method for the determination of hydrogen peroxide and glucose with  $\text{Fe}_3\text{O}_4$  as catalyst, *Talanta*, 2011, **85**, 1075–1080.
- 311 Y.-I. Dong, H.-G. Zhang, Z. U. Rahman, I. Su, X.-J. Chen, J. Hu and X.-G. Chen, Graphene oxide- $\text{Fe}_3\text{O}_4$  magnetic nanocomposites with peroxidase-like activity for colorimetric detection of glucose, *Nanoscale*, 2012, **4**, 3969–3976.
- 312 Q. Liu, L. Zhang, H. Li, Q. Jia, Y. Jiang, Y. Yang and R. Zhu, One-pot synthesis of porphyrin functionalized  $\gamma\text{-Fe}_2\text{O}_3$  nanocomposites as peroxidase mimics for  $\text{H}_2\text{O}_2$  and glucose detection, *Mater. Sci. Eng., C*, 2015, **55**, 193–200.
- 313 Y. Wang, B. Zhou, S. Wu, K. Wang and X. He, Colorimetric detection of hydrogen peroxide and glucose using the magnetic mesoporous silica nanoparticles, *Talanta*, 2015, **134**, 712–717.
- 314 Q. Chang and H. Tang, Optical determination of glucose and hydrogen peroxide using a nanocomposite prepared from glucose oxidase and magnetite nanoparticles immobilized on graphene oxide, *Microchim. Acta*, 2014, **181**, 527–534.
- 315 M. I. Kim, J. Shim, T. Li, J. Lee and H. G. Park, Fabrication of Nanoporous Nanocomposites Entrapping  $\text{Fe}_3\text{O}_4$  Magnetic Nanoparticles and Oxidases for Colorimetric Biosensing, *Chem.-Eur. J.*, 2011, **17**, 10700–10707.
- 316 M. I. Kim, J. Shim, T. Li, M.-A. Woo, D. Cho, J. Lee and H. G. Park, Colorimetric quantification of galactose using a nanostructured multi-catalyst system entrapping galactose oxidase and magnetic nanoparticles as peroxidase mimetics, *Analyst*, 2012, **137**, 1137–1143.
- 317 M. I. Kim, J. Shim, H. J. Parab, S. C. Shin, J. Lee and H. G. Park, A convenient alcohol sensor using one-pot nanocomposite entrapping alcohol oxidase and magnetic nanoparticles as peroxidase mimetics, *J. Nanosci. Nanotechnol.*, 2012, **12**, 5914–5919.
- 318 S. Singh, Nanomaterials Exhibiting Enzyme-Like Properties (Nanozymes): Current Advances and Future Perspectives, *Front. Chem.*, 2019, **7**, 46.
- 319 D. Duan, K. Fan, D. Zhang, S. Tan, M. Liang, Y. Liu, J. Zhang, P. Zhang, W. Liu and X. Qiu, Nanozyme-strip for rapid local diagnosis of Ebola, *Biosens. Bioelectron.*, 2015, **74**, 134–141.
- 320 M. S. Kim, S. H. Kweon, S. Cho, S. S. A. An, M. I. Kim, J. Doh and J. Lee, Pt-Decorated Magnetic Nanozymes for Facile and Sensitive Point-of-Care Bioassay, *ACS Appl. Mater. Interfaces*, 2017, **9**, 35133–35140.
- 321 N. Cheng, C. Zhu, Y. Wang, D. Du, M.-J. Zhu, Y. Luo, W. Xu and Y. Lin, Nanozyme Enhanced Colorimetric Immunoassay for Naked-Eye Detection of Salmonella Enteritidis, *J. Anal. Test.*, 2019, **3**, 99–106.
- 322 H. Y. Shin, B.-G. Kim, S. Cho, J. Lee, H. B. Na and M. I. Kim, Visual determination of hydrogen peroxide and glucose by exploiting the peroxidase-like activity of magnetic nanoparticles functionalized with a poly(ethylene glycol) derivative, *Microchim. Acta*, 2017, **184**, 2115–2122.
- 323 L. Zhang, R. Huang, W. Liu, H. Liu, X. Zhou and D. Xing, Rapid and visual detection of *Listeria monocytogenes* based on nanoparticle cluster catalyzed signal amplification, *Biosens. Bioelectron.*, 2016, **86**, 1–7.
- 324 W. Li, G.-C. Fan, F. Gao, Y. Cui, W. Wang and X. Luo, High-activity  $\text{Fe}_3\text{O}_4$  nanozyme as signal amplifier: A simple, low-cost but efficient strategy for ultrasensitive photoelectrochemical immunoassay, *Biosens. Bioelectron.*, 2019, **127**, 64–71.
- 325 L. Tian, J. Qi, O. Oderinde, C. Yao, W. Song and Y. Wang, Planar intercalated copper (II) complex molecule as small molecule enzyme mimic combined with  $\text{Fe}_3\text{O}_4$  nanozyme for bienzyme synergistic catalysis applied to the microRNA biosensor, *Biosens. Bioelectron.*, 2018, **110**, 110–117.
- 326 T. Li, P. Hu, J. Li, P. Huang, W. Tong and C. Gao, Enhanced peroxidase-like activity of  $\text{Fe}@PCN-224$  nanoparticles and their applications for detection of  $\text{H}_2\text{O}_2$  and glucose, *Colloids Surf., A*, 2019, **577**, 456–463.
- 327 R. Zhang, N. Lu, J. Zhang, R. Yan, J. Li, L. Wang, N. Wang, M. Lv and M. Zhang, Ultrasensitive aptamer-based protein assays based on one-dimensional core-shell nanozymes, *Biosens. Bioelectron.*, 2020, **150**, 111881.
- 328 W. Yang, J. Li, M. Wang, X. Sun, Y. Liu, J. Yang and D. H. Ng, A colorimetric strategy for ascorbic acid sensing based on the peroxidase-like activity of core-shell  $\text{Fe}_3\text{O}_4/\text{CoFe-LDH}$  hybrid, *Colloids Surf., B*, 2020, **188**, 110742.
- 329 X. Wang, Y. Hu and H. Wei, Nanozymes in bionanotechnology: from sensing to therapeutics and beyond, *Inorg. Chem. Front.*, 2016, **3**, 41–60.
- 330 L. Gao, X. Yan and X. Nanozymes, an emerging field bridging nanotechnology and biology, *Sci. China: Life Sci.*, 2016, **59**, 400–402.
- 331 D. Jiang, D. Ni, Z. T. Rosenkrans, P. Huang, X. Yan and W. Cai, Nanozyme: new horizons for responsive biomedical applications, *Chem. Soc. Rev.*, 2019, **48**, 3683–3704.
- 332 J. Wu, X. Wang, Q. Wang, Z. Lou, S. Li, Y. Zhu, L. Qin and H. Wei, Nanomaterials with enzyme-like characteristics (nanozymes): next-generation artificial enzymes (II), *Chem. Soc. Rev.*, 2019, **48**, 1004–1076.
- 333 Y. Meng, W. Li, X. Pan and G. M. Gadd, Applications of nanozymes in the environment, *Environ. Sci.: Nano*, 2020, **7**, 1305–1318.
- 334 W. Li, G. C. Fan, F. Gao, Y. Cui, W. Wang and X. Luo, High-activity  $\text{Fe}_3\text{O}_4$  nanozyme as signal amplifier: A simple, low-cost but efficient strategy for ultrasensitive photoelectrochemical immunoassay, *Biosens. Bioelectron.*, 2019, **127**, 64–71.
- 335 Y. Guo, Y. Tao, X. Ma, J. Jin, S. Wen, W. Ji, W. Song, B. Zhao and Y. Ozaki, A dual colorimetric and SERS detection of  $\text{Hg}^{2+}$  based on the stimulus of intrinsic oxidase-like catalytic activity of  $\text{Ag-CoFe}_2\text{O}_4/\text{reduced graphene oxide}$  nanocomposites, *Chem. Eng. J.*, 2018, **350**, 120–130.
- 336 T. Qin, R. Ma, Y. Yin, X. Miao, S. Chen, K. Fan, J. Xi, Q. Liu, Y. Gu, Y. Yin, J. Hu, X. Liu, D. Peng and L. Gao, Catalytic



- inactivation of influenza virus by iron oxide nanozyme, *Theranostics*, 2019, **9**, 6920–6935.
- 337 J. Jiang, C. He, S. Wang, H. Jiang, J. Li and L. Li, Recyclable ferromagnetic chitosan nanozyme for decomposing phenol, *Carbohydr. Polym.*, 2018, **198**, 348–353.
- 338 M. Huo, L. Wang, Y. Chen and J. Shi, Tumor-selective catalytic nanomedicine by nanocatalyst delivery, *Nat. Commun.*, 2017, **8**, 357.
- 339 P. Boruah and M. Das, Dual responsive magnetic Fe<sub>3</sub>O<sub>4</sub>-TiO<sub>2</sub>/graphene nanocomposite as an artificial nanozyme for the colorimetric detection and photodegradation of pesticide in an aqueous medium, *J. Hazard. Mater.*, 2019, **385**, 121516.
- 340 A. Nsabimana, S. A. Kitte, F. Wu, L. Qi, Z. Liu, M. N. Zafar, R. Luque and G. Xu, Multifunctional magnetic Fe<sub>3</sub>O<sub>4</sub>/nitrogen-doped porous carbon nanocomposites for removal of dyes and sensing applications, *Appl. Surf. Sci.*, 2019, **467**, 89–97.
- 341 M. Wang, N. Wang, H. Tang, M. Cao, Y. She and L. Zhu, Surface modification of nano-Fe<sub>3</sub>O<sub>4</sub> with EDTA and its use in H<sub>2</sub>O<sub>2</sub> activation for removing organic pollutants, *Catal. Sci. Technol.*, 2012, **2**, 187–194.
- 342 F. Chen, S. Xie, X. Huang and X. Qiu, Ionothermal synthesis of Fe<sub>3</sub>O<sub>4</sub> magnetic nanoparticles as efficient heterogeneous Fenton-like catalysts for degradation of organic pollutants with H<sub>2</sub>O<sub>2</sub>, *J. Hazard. Mater.*, 2017, **322**, 152–162.
- 343 C. Xiao, J. Li and G. Zhang, Synthesis of stable burger-like  $\alpha$ -Fe<sub>2</sub>O<sub>3</sub> catalysts: Formation mechanism and excellent photo-Fenton catalytic performance, *J. Cleaner Prod.*, 2018, **180**, 550–559.
- 344 M. Mahmoudi, A. Simchi, M. Imani and U. O. Häfeli, Superparamagnetic iron oxide nanoparticles with rigid cross-linked polyethylene glycol fumarate coating for application in imaging and drug delivery, *J. Phys. Chem. C*, 2009, **115**, 9325–9335.
- 345 D. L. Thorek, A. K. Chen, J. Czupryna and A. Tsourkas, Superparamagnetic iron oxide nanoparticle probes for molecular imaging, *Ann. Biomed. Eng.*, 2006, **34**, 23–38.
- 346 B. Szalay, E. Tátrai, G. Nyírő, T. Vezér and G. Dura, Potential toxic effects of iron oxide nanoparticles in *in vivo* and *in vitro* experiments, *J. Appl. Toxicol.*, 2012, **32**, 446–453.

